THE EFFECT OF DEFORMATION ON DISPERSION HARDENED ALLOYS

NGR 36-003-094

FINAL REPORT

November 1967

Prepared by: G.S. Doble, L. Leonard and L.J. Ebert

Submitted to:

OFFICE OF GRANTS AND RESEARCH CONTRACTS
ATTENTION: Code SC
NATIONAL AERONAUTICS AND SPACE ADMINISTRATION
WASHINGTON, D.C. 20546

DEPARTMENT OF METALLURGY

CASE WESTERN RESERVE UNIVERSITY

CLEVELAND, OHIO 44106

ABSTRACT

The elevated temperature tensile properties of TD Nickel were measured after mechanical working and recrystallization treatments. Increases in strength were produced by cold swaging while upset forging or prior torsion lowered the strength. Recrystallization to a coarse grain size increased strength over the fine grained cold worked bar stock. Activation energies, measured at 2000°F under tensile conditions, ranged from 160 to 330 K-cal/mol for both fine grained cold worked or coarse grained recrystallized structures. Intercrystalline cracking was the controlling mechanism for elevated temperature strength of recrystallized TD Nickel. Evidence for a similar mechanism in fine grained TD Nickel is discussed.

The development of a recrystallization resistent structure in TD Nickel was shown to depend upon the deformation history. Comparable percentages of cold deformation produced recrystallization temperatures ranging from 1250° to above 2400°F depending upon working operation and direction. No recrystallization took place after cold swaging reductions of 15 - 95% while the occurrence and extent of recrystallization after a given cold rolling reduction varied with the rolling direction. In some cases increasing amounts of deformation, in addition to causing increased strain hardening, were effective in increasing the recrystallization temperature. Recrystallization resistance was accompanied by the development of relatively sharp crystallographic textures.

FOREWARD

This Final Report covers work performed under Grant NGR 36-003-094 from 1 October 1966 to 30 November 1967. The data presented were submitted to Case Western Reserve University by one of the authors (GSD) in partial fulfullment of the requirements for the degree of Doctor of Philosophy.

TABLE OF CONTENTS

LIST OF TABLES

LIST OF FIGURES

LIST OF FIGURES CON'T

LIST OF FIGURES CON'T

TABLE OF SYMBOLS

γ = shear strain

r = bar radius

θ = angle of twist

l = bar length

$\dot{\epsilon}$ = strain rate

A = frequency factor

ΔH = activation energy

s = structure factor

σ = flow stress

σ_G = internal stress

$\sigma_{.2YS}$ = 0.2% offset yield stress

T = absolute temperature

R = universal gas constant

G = shear modulus

INTRODUCTION

The incorporation of a fine hard particle second phase in a single phase matrix results in an alloy which is useful to a much higher fraction of its melting point than conventional alloys. The inherent high temperature stability of dispersion hardened alloys of nickel and cobalt is presently of great commercial interest in the so-called 1900° - 2400°F materials gap, the range above general super-alloy capabilities and below normal refractory metal application. However, the technology of producing dispersion hardened alloys has outstripped an understanding of the properties of these materials.

The objectives of the present investigation were to investigate the mechanisms of strengthening and recrystallization in a commercial dispersion hardened material. Since these topics were evaluated in two parallel studies, the results are presented in two parts. The strengthening mechanisms at elevated temperatures will be discussed first and the recrystallization behavior presented next.

STRENGTHENING MECHANISMS

INTRODUCTION

The primary advantage of dispersion hardened alloys over conventional materials is the stability of high temperature strength. However, the mechanisms of strengthening in these materials are not well established. Although theories describing the influence of a hard particle dispersed phase on yield strength and flow stress have been reviewed by several authors (1,2,3,4), most of these theories have treated idealized conditions of unworked single crystals at low temperatures. At present there is no agreement upon a single theory applicable to yielding and flow of commercial dispersion hardened alloys which are cold worked, polycrystalline, and used at elevated temperatures. It is generally acknowledged that the elevated temperature strength of a dispersion hardened alloy includes contributions from the presence of the dispersed particles, which strengthen the matrix by acting as dislocation barriers, and from the development and retention of a particle-stabilized as-worked structure. TD Nickel provides an example of the difficulty of applying these general concepts to strength changes in a commercial dispersion hardened alloy.

If TD Nickel powder is warm extruded to a fully dense structure, the elevated temperature yield and tensile strengths are initially quite low, but may be increased by a factor of three or four by cold swaging (5). On this basis, it would appear that only particle strengthening is active in the as-extruded material while

a cold working contribution is included for the swaged bar. However, if the swaged bar is cold rolled and recrystallized, the yield and tensile strengths are still high. Since the yield strength of a fully recrystallized structure should also be due only to particle strengthening, the dislocation density being appreciably reduced by recrystallization (6), it is not clear why the as-extruded and recrystallized strengths differ. The behavior is not confined to the TD Nickel system,since similar increases in elevated temperature strength with recrystallization of an as-extruded structure to a coarse grain size have been reported in TD Nickel-Chromium, TD Nickel-Molybdenum (7), and for creep of SAP (8).

It also appears that the strengthening of TD Nickel by swaging is not due to a simple process such as strain hardening the nickel matrix. This is illustrated by the observation that transverse elevated temperature yield and tensile strengths are very low in the swaged condition regardless of the longitudinal strength level. Another argument against a simple strain hardening viewpoint is that upset forging commercial TD Nickel bar by 50%, a cold working process, will reduce the elevated temperature strength by half (5). No obvious defects in the microstructure, such as seams or cracks, were found to explain these low strength values. It therefore appears that while cold working operations may produce strong as-worked materials, the specific structure produced is intimately related to the working process and direction rather than to the amount of deformation.

DESIGN OF THE STUDY

The objectives of the study were to examine, quantitatively, the effect of mechanical working and recrystallization on the elevated temperature tensile properties of TD Nickel and to evaluate potential mechanisms affecting these properties. The mechanical working operations consisted of swaging, upset forging, and torsion. This combination of deformation processes includes elongation, compression, and twisting of a metal grain which are the basic modes of shape change. Mechanical working was the only variable operating during this portion of the study since no recrystallization could be induced after the working operations employed. The independent variables were the amount of working and the stress state of the working operation while the dependent variables were the 2000°F tensile properties.

The recrystallized structures were produced by annealing either an as-extruded or as-extruded-plus-rolled condition, with the latter condition producing a greater degree of recrystallization. The majority of the effort was in evaluating the effect of prior working operations on the properties of the recrystallized structure but a few tests were performed after subsequent working of the recrystallized structure.

Investigation of the mechanisms of yielding and flow was partially phenomenological, through use of activation energy measurements, and partially physical with replica electron microscopic observations of specimens strained to the yield point. The

activation energy measurements would indicate if the rate controlling mechanism during tensile deformation changed with grain size. Such a change has been proposed (9) to explain the differences in creep of fine (8,10) and coarse (8) grained SAP and nickel-thoria alloys (11). Creep of coarse grained alloys is felt to be controlled by climb with an activation energy equal to matrix self diffusion. Creep of fine grained materials has been variously interpreted as being controlled by grain boundary dislocation generation (8), or in TD Nickel, grain boundary sliding (12) with activation energies several times the value for matrix self-diffusion.

Direct observations of the structural changes that occur with tensile deformation were made by light and replica electron microscopy. Specimens examined included fractured tensile specimens and tensile specimens strained to various points on the stress strain curve and then unloaded. A few observations were made on the surfaces of recrystallized tensile specimens strained to the yield point to observe if grain boundary sliding was taking place.

MATERIAL

The two types of TD Nickel selected for the study, as-extruded and commercial bar, originated from a single sintered billet but were taken from different stages of the manufacturing process. TD Nickel is made by the chemical production of a thoria containing nickel powder, the compaction and sintering of this powder into billets, and the consolidation of this billet by warm extrusion (13). After extrusion, a length of the three-inch diameter extruded round was cut off to serve as the "as-extruded" material for the present study. The as-extruded condition, which is presently not used commercially because of low elevated temperature strength, was employed as a reference material containing a minimum amount of mechanical working. The microstructure, shown in Figure 1, consisted of elongated grains about 2 microns by 4 microns in size. The hardness was 85 R_G. Changes in hardness and X-ray line breadth with annealing indicated that the material was in a cold worked condition.

The balance of the extruded material was cold worked to commercial one inch bar stock by the supplier* using a proprietary working schedule** and a final stress relief anneal. The microstructure of this material, Figure 2, revealed that the grains had been considerably elongated by the working process, the grain size being 1 micron by 15 microns. The hardness was 82 R_G. The commercial bar

---

* The DuPont Company

** Details not available.

was in a cold worked state since annealing above 2000°F resulted in a hardness drop without any observable change in the microstructure. The chemical composition is listed in Table I. Thoria content was 2.4% by weight which is approximately the same by volume. The average particle size of commercial TD Nickel bar has been reported as 370Å (12).

EXPERIMENTAL PROCEDURE

The working operations selected for the program were swaging, upset forging, and torsion. Swaging samples of as-extruded material were prepared by slitting a length of the extrusion into quarters and machining the quarters to one inch diameter. As-extruded and one inch commercial bar were then both cold swaged in passes of 15% to a total reduction of 95% in cross sectional area with lengths cut off at intermediate reductions. No intermediate stress relief was employed and neither type of bar showed a tendency for cracking during swaging. Tensile specimens were sectioned from quarter, half, or full cross sections depending upon the swaged diameter.

Upset forging was performed on slugs of one inch diameter bar stock with ends faced parallel. Starting lengths were adjusted to give a final one inch height after upsetting reductions of 15, 35, or 50%. Upset forging was performed between flat dies in a 150 ton hydraulic forge press. A graphite-grease lubricant was coated on the dies before forging. Forging at elevated temperatures employed heating for 20 to 30 minutes in air. Barreling was observed on all specimens but was less pronounced at the elevated temperature. After forging, the samples were slit in half and a longitudinal or transverse tensile specimen taken from each half as close to the center line of the bar as possible.

Specimens deformed in torsion had a gage section of 0.187" diameter by 0.850" and were twisted in a special torsion tester

constructed from a lathe bed. Specimens were twisted to plastic deflections of 120° to 240° at room temperature. The strain gradient in a twisted bar is linear and the shear strain (γ) goes from zero at the center to a maximum value $\gamma = \frac{r\theta}{L}$ at the surface. A 240° twist corresponds to a γ of 0.52. Longitudinal lines scribed on the specimen surface indicated that strain was uniform during twisting and untwisting. Specimens were then machined to 0.173" diameter to insure axiality and tested in tension at 2000°F.

Recrystallization heat treatments, where employed, were performed on specimen blanks before machining in a platinum wound tube furnace with the temperature controlled to $\pm$ 5°F with an atmosphere of flowing argon.

Tensile testing was performed in air on a standard Instron Tensile Machine using a constant crosshead speed. Yield and tensile strengths at elevated temperatures were determined from load-deflection curves recorded during the test. At room temperature, an extensometer was used through the yield point and concentric alignment fixtures were employed. Elongation measurements were made on an optical comparator and the reduction in area determined by measuring the diameter after fracture at two places 90° apart with pointed micrometers. A few proportional limit measurements were made at room temperature using strain gages. All specimens were held at test temperatures 15 minutes prior to test. The temperature gradient along the gage length of the specimen was less than 5°F. Stress rupture tests were performed in air on a standard Arcweld stress-rupture frame. Specimens were soaked two to

four hours to stabilize any temperature gradients. Test temperatures were controlled to $\pm$ 7°F.

Room temperature tests were made with threaded specimens containing a gage section of 0.160" diameter by 1.25". At 2000°F it was necessary to reduce the gage diameter to 0.113" to avoid failure of the threads. Sub-size specimens having a gage section of 0.080" diameter by 0.400 long were used to compare longitudinal and transverse properties or in situations where limited material was available. Specimen size is indicated in all tables.

Activation energy measurements were made on as-extruded, commercial bar, and a recrystallized material. The recrystallized structure was produced by sectioning a slab 1/2" thick by 3" wide by 6" long from the as-extruded round and cold rolling in 15% passes to 47% reduction in thickness with the rolling direction parallel to the extrusion axis. The rolled piece was then heat treated one hour at 2300°F in an atmosphere of argon and tensile specimens machined parallel to the rolling direction. Longitudinal tensile blanks of the as-extruded material were cut from within one inch of the center of the section and also heat treated one hour at 2300°F in argon. Tensile specimens were machined from the center line of the commercial bar after a 2300°F anneal.

The determination of activation energy for tensile yielding was performed by two different test methods, a conventional test method and a differential test method, both of which are described by Conrad (14). The activation energy determined by both methods is

defined in the general equation:

$$\dot{\epsilon} = A(\sigma, T, s)\, e^{-\frac{\Delta H(\sigma, T, s)}{RT}} \qquad \text{Eqn (1)}$$

In calculating ΔH, it is necessary to assume that A is not a function of temperature.

The "conventional" test method employs standard constant strain rate tensile tests to measure yield and flow stress as a function of temperature. The stress for a given strain, such as the 0.2% offset yield stress , is then plotted as a function of temperature for several strain rates. The stress at a very low strain is used in order that the structure be essentially unchanged from the initial condition, thus providing a constant s value in Equation (1). At a constant stress level, the activation energy in Equation (1) may be written as

$$\Delta H = -R \left(\frac{\partial \ln \dot{\epsilon}}{\partial 1/T} \right)_{\sigma, s} \qquad \text{Eqn. (2)}$$

The activation energy calculated by Equation (2) could conceivably vary with stress, but reported activation energies for TD Nickel in creep indicate no stress dependence at elevated temperatures (1).

The differential test method employs an abrupt change in strain rate during the tensile test. If the change is effected rapidly enough, the structure will remain constant and the measured change in stress will be related to the deformation mechanism. The activation energy is obtained from differential tests through the equation

$$\Delta H = -T^2 R \left(\frac{\partial \ln \dot{\epsilon}}{\partial \sigma} \right)_{T, s} \left(\frac{\partial \sigma}{\partial T} \right)_{\dot{\epsilon}, s} \qquad \text{Eqn. (3)}$$

An expression for the activation energy similar to Equation (3), but corrected for the change in shear modulus with temperature, is

$$\Delta H = -RT^2 \left(\frac{\partial \ln \dot{\epsilon}}{\partial \sigma}\right)_T \left[\left(\frac{\partial \sigma}{\partial T}\right)_{\dot{\epsilon}} - \left(\frac{\sigma_G}{G}\frac{dG}{dT}\right)\right] \qquad \text{Eqn. (4)}$$

where σ_G is the internal stress and G is the shear modulus. Using shear modulus data of nickel from the literature (15), and substituting $\sigma_{.2YS}$ for σ_G, the maximum correction is about 20%. However, since the yield stress (corrected for modulus variation with temperature) versus temperature curve did not level off to a constant value, the thermal component is not negligible and the substitution of $\sigma_{.2YS}$ for σ_G (16) is probably not justified; consequently, the full correction does not apply. For this reason, no correction was used in this program.

To examine the structural changes occurring as a function of tensile strain, some tensile tests were run to pre-determined points on the stress strain curve, the test stopped, the specimen unloaded, removed from the testing furnace and cooled to room temperature. Several recrystallized specimens were tested in a similar way in a vacuum of 1×10^{-5} torr. Prior to test, these recrystallized specimens were electropolished and circumferential scratches placed on the surface with metallographic paper.

Metallographic preparation for examination by light microscopy employed standard metallographic polishing with a 1:1 acetic-nitric etch. Specimens for electron microscopy were electropolished in a 1:7 sulfuric methanol solution and chromium shadowed collodion replicas prepared.

RESULTS

A. Base Line Tensile Properties

2000°F

The 2000°F tensile properties, summarized in Table 2, show that the as-extruded material is weak in both test directions with a very slight directionality apparent between the longitudinal and transverse strength values. The commercial bar is strong in the longitudinal direction and weak when tested at 45° or transverse to the bar axis. Low strength values of both as-extruded and commercial bar materials are accompanied by high values of measured ductility.

Load-extension curves for the 2000°F tests of Table 2 are plotted in Figure 3. The longitudinal test curve of the commercial bar shows a very high yield strength but exhibits little work hardening. Fracture occurred at a low value of extension. The transverse test curves for both materials, and the longitudinal as-extruded curve, show yielding at very low loads with subsequent constant load extension over a very wide range of tensile strains. The three curves are very similar in shape, differing only in total elongation. The apparent lower modulus for the three lower strength tests is a reproducible phenomenon at elevated temperatures.

The high elongations represented by the curves in Figure 3 are not true measures of ductility because of the incidence of internal cracking. The differences between true ductility and measured ductility has been discussed in the literature (17). Metallographic examination of the specimens after testing revealed an extensive

room temperature strength correlated with the room temperature hardness. The only property influenced by the direction of testing was the reduction in area which was lower in the transverse direction. This is a normal relationship for mechanically fibered materials.

Stability

One hour exposures to temperatures up to 2500°F had no measurable effect on the 2000°F tensile properties nor did a 2300°F anneal change the 2000°F tensile properties of as-extruded material. However, elevated temperature annealing did affect the room temperature hardness and strength of both materials, as is shown in Table 3. The changes are generally typical of a conventional recovery process with a decrease in strength and an increase in ductility, particularly the elongation. Once again it should be emphasized that factors influencing room temperature strength do not necessarily affect elevated temperature properties.

B. Mechanical Working

Mechanical working operations were performed on both as-extruded and commercial bar. Both of these materials were fine grained after testing, indicating that recrystallization had occurred neither during warm working nor during tensile testing at 2000°F. No cracks or imperfections were noted after working to account for the property changes to be discussed.

Swaging

Tensile properties of as-extruded TD Nickel cold swaged various amounts and tested at 2000°F are listed in Table 4. Swaging has increased the yield and tensile strengths by a factor of 4. The

degree of internal cracking, Figure 4. The cracking is also the source of the large reduction in area reported for the transverse test of commercial bar. The unusual fracture appearance of the test pieces is illustrated in Figure 5. The cross section of the tensile fracture was elliptical with the major axis in the fiber direction. Virtually no reduction had taken place in the fiber direction. The entire length of the tensile specimen has this approximate dimension, and the effect is not confined to strains after the ultimate load. The surface cracks in the oxide layer illustrate that deformation has been localized to two sides of the specimen.

The direction of the internal cracks found in fracture tensile specimens followed the direction of the grain boundaries. Figure 6 illustrates the direction of cracking encountered for three different test directions of commercial bar. Little cracking is apparent for the longitudinal tests while the 45^{o} test and transverse tests have cracks at 45^{o} and 90^{o} respectively. Such cracking has previously been found in creep of TD Nickel and the cracks were reported to be intercrystalline (12).

Room Temperature.

The room temperature tensile properties of as-extruded and commercial bar materials show very little directionality in strength values. In contrast to the elevated temperature strength, the room temperature strength is very similar for the two materials, with the as-extruded strength being slightly higher. The point should be made here, emphatically, that there was no relationship found between room temperature and elevated temperature strength. In general, the

yield and tensile strengths, plotted against true strain during swaging in Figure 7, show a linear strength increase up to a swaging reduction of 90%, a true strain of 2.2. Further deformation does not appreciably add to the strength. This behavior is typical of a strain hardened material in that lower reductions provide a much greater strength increment. A swaging reduction of at least 90% is required to raise the strength of as-extruded material to the level of commercial bar. As the strength level is increased, the corresponding ductility values show a steady decrease. The reason for the abrupt lowering of ductility at 26% reduction is not known although the data were obtained in duplicate.

Tensile properties of commercial TD Nickel bar given various swaging treatments are listed in Table 5. A strengthening increase of approximately 25% is produced with a slight decrease in ductility. As with the higher reduction of the as-extruded material, the strength increment levels off at high reductions.

Upset Forging

The longitudinal and transverse 2000°F strength properties after upset forging are summarized in Figure 8 and listed in Table 6. Upset working reduces the longitudinal yield and tensile strengths, but does not influence the transverse strength. Unlike the change in as-swaged strength, the decrease in strength with true upsetting strain does not follow a linear plot. By 50% reduction, the longitudinal and transverse strengths have reached the same low value. While some scatter exists, the measured ductility in the longitudinal direction increases as the strength decreases. The measured

transverse ductility remains high regardless of the amount of upset. Again, the measured ductility includes a considerable contribution from internal cracking. Forging temperatures ranging from room temperature to 2000°F did not affect the tensile properties at a 50% reduction. The room temperature hardness after a 50% upset at room temperature increased $2\frac{1}{2}$ R_G points indicating that strain hardening did occur with deformation.

The load-extension curves from 2000°F longitudinal tensile tests after a number of room temperature upsetting reductions are shown in Figure 9. Increased reduction has lowered the yield and tensile strengths but increased the elongation appreciably. After forging reduction of 50% the tensile curve is virtually indistinguishable from the as-extruded material. An apparent lowering of the modulus is also found with increasing reduction.

The internal cracking present after a 2000°F longitudinal tensile test in a sample upset 50% at room temperature is illustrated in Figure 10. The cracks are normal to the applied stress, indicating that some grain boundaries exist transverse to the original bar axis, for example compare to Figure 6. The upsetting operation has evidently introduced some buckling of the grains.

Torsion

The influence of torsional prestrain on the 2000°F tensile properties of commercial TD Nickel bar is illustrated in Table 7. Specimens were twisted at room temperature and tested in tension at 2000°F. The tensile test results show that relatively small torsional strains reduce the yield and tensile strengths appreciably, but the

measured ductility was not affected. If a specimen was twisted and then untwisted, the torsional prestrain affected neither the ductility nor the strength. Restoration of strength after untwisting indicates that some reversible feature of the twisted geometry has reduced strength. Similar results have been reported for room temperature testing of steel (18) and nickel (19). The results for steel have been explained in terms of the alignment of segregation cavities or various impurity phases. For pure nickel it was necessary to postulate the presence of longitudinal micro cracks. Neither of the explanations is plausible for TD Nickel since neither gross impurities nor pre-existing cracks are reported for this material. The most probable mechanism in TD Nickel is the failure of grain boundaries inclined to the axis of applied stress.

C. Recrystallization

All recrystallized specimens were prepared from an as-extruded starting condition, either by working plus annealing or by annealing alone. In both instances the recrystallized grain size is about .05 to .1 mm by 1 mm, contrasted to the 1-2 micron by 4-15 micron of the as-extruded or commercial bar materials. The recrystallized grains were always elongated in the direction of maximum prior work, generally the extrusion or bar direction, although cross working did decrease their longitudinal dimension. A typical recrystallized structure is shown in Figure 11.

Recrystallized by Annealing Alone.

Samples of as-extruded material were recrystallized by

annealing one hour at 2500°F in an atmosphere of flowing argon. This treatment has the disadvantage that thoria may have coarsened during annealing above 2450°F (20). The resultant microstructure was 50-70% recrystallized with an elongated but coarse grain shape. The longitudinal tensile properties of the recrystallized structure, Table 8, compared to the cold worked as-extruded condition in Table 2, show a sharp increase in the yield and tensile strengths. The reduction in area remains high while the elongation is reduced. Testing at 45° or transverse to the original extrusion axis (which is also 45° or transverse to the length dimension of the recrystallized grains) reduces the strength to much the same degree as the fine grained commercial bar. The ductility values are all much reduced in the transverse direction.

Recrystallized by rolling plus annealing.

Rolling deformation of TD Nickel is particularly effective in producing a recrystallized structure upon subsequent annealing. A larger degree of recrystallization may be produced and lower annealing temperatures may be employed, thus eliminating the possibility of thoria coarsening. The structure produced by rolling a slab to a reduction of 51% parallel to the extrusion axis is 100% recrystallized. The tensile properties of this structure are listed in Table 8. The strength values are even higher than those of the commercial cold worked bar stock. The recrystallized specimen has a large reduction in area but only moderate elongation. Intercrystalline fractures were noted in all tests of recrystallized material. On testing at an angle to the grains or across the grains, the

strength is still high but the ductility is nil. Load-deflection curves of longitudinal and transverse tests, compared in Figure 12, show that the transverse test pieces fail in a brittle manner.

The superiority of the recrystallized structure in 2000°F tensile strength is also maintained in elevated temperature stress rupture behavior. Stress rupture life as a function of applied stress is plotted in Figure 13 for recrystallized and commercial bar materials at 1950°F. The recrystallized material has a 100 hour rupture stress of 16,000 psi compared to a 12,000 psi stress for commercial bar.

Effect of Rolling Direction

Since the properties of TD Nickel are sensitive to the direction of working, the influence of prior rolling direction on recrystallized strength was established. As-extruded slabs were rolled to a reduction of 50% with the rolling direction either longitudinal, transverse, or alternately longitudinal and transverse to the extrusion axis. The tensile properties of these materials, tested in the extrusion direction, are shown in Table 8 after a recrystallization treatment of one hour at 2400°F. Rolling in the longitudinal direction has produced the highest strength, with rolling alternately longitudinal and transverse being almost the same. Rolling in the transverse direction appreciably lowers the strength. The reduction in area drops off in the same order. The two recrystallized structures are shown in Figure 14. The strength changes correlate with the degree of fibering of the recrystallized

grains.

Effect of Cold Work on Recrystallized Strength.

The effect of a 50% cold swaging reduction upon the strength of a recrystallized structure is shown in Table 9. There is little if any increase in strength although the change in specimen size slightly complicates the comparison. The differences in elongation may be explained by the different gage sections rather than differences in material properties.

D. Activation Energy

The temperature dependence of activation energy was determined for commercial TD Nickel bar using the conventional test method. The tensile specimens used had been machined for a prior study and were taken from another heat of material. These particular specimens are the only material used in the present study which did not originate from the single billet described in the MATERIALS section. This prior heat had an analysis of 2.3% thoria with an average particle size appreciably larger than the present material. Tensile tests were run at temperatures ranging from ambient to 2000°F at strain rates of 5×10^{-2} and 5×10^{-3} min^{-1} using a specimen gage section 0.080" dia. x 0.400" length.

Activation energies, calculated from plots of yield strength versus temperature, were determined at various constant stress levels. The resultant activation energies are plotted against homologous temperature in Figure 15. At low and intermediate temperatures, activation energies are all less than the 61-67 K-cal/mole

values reported for self diffusion of pure nickel. This is consistent with a process such as cross slip controlling yielding. The activation energy increases above about 0.65 of the melting point, reaching a value twice the activation energy for self diffusion at 0.8 of the melting point, (2000°F). Activation energies for two SAP alloys plotted in the same figure follow a similar trend. An increase in the activation energy at elevated temperatures has also been reported for commercial TD Nickel bar in creep with a crossover point between high and low temperatures activation energies of about 1/2 of the melting point (12). There is no generally accepted explanation of the very high activation energies at elevated temperatures.

The precision of the activation energies reported in Figure 15 is not particularly good at elevated temperatures since only two strain rates were used and a limited number of specimens were available. The small gage section is another problem in accurate determination of yield strength from a load-deflection curve. There are also possible errors in using the calculation of Equation 2 over a wide temperature range. The internal stress field may be larger at lower temperatures and the activation energy may be stress dependent. However, even with these limitations in mind, it is obvious that different activation mechanisms are operative at low and high temperatures. It is also apparent that similarities exist between the mechanisms operative in tensile deformation of TD Nickel and SAP alloys.

Activation Energy as a Function of Structure

The activation energy for three different structural conditions of TD Nickel was determined near 2000°F using both the conventional and the differential test methods. Materials tested were as-extruded + 1 hr/2300°F, commercial bar + 1 hr/2300°F, and a recrystallized structure produced by a 47% longitudinal rolling reduction of as-extruded material + 1 hr/2300°F. The 2300°F anneal was given to all materials in order to provide a common thermal history for both recrystallized and unrecrystallized materials. All specimens were taken in the longitudinal direction.

The results of tensile testing are listed in Table 10 and the yield and tensile strengths plotted against test temperature in Figures 16, 17 and 18. The data are consistent and plot as parallel lines in most cases. Calculations of activation energy made from Figures 16, 17, and 18 are listed in Table 11 under the conventional test method heading. The activation energies for the fine grained materials, based on the strain at 0.2% offset, are 193 K-cal/mol for the extruded material and 220 K-cal/mol for the commercial bar. These values are in fairly good agreement with one another. The recyrstallized material has a higher activation energy of 330 K-cal/mol.

Activation energies determined by the differential method are also listed in Table 11. Each value listed in Table 11 is the average of two tests, one between 1.6×10^{-3} to 1.6×10^{-2} min^{-1} strain rate and a second at 1.6×10^{-2} to 1.6×10^{-1} min^{-1} strain rates. No consistent difference in activation energy between the two pairs of

strain rates was noted.

The activation energy for self diffusion of nickel is given as 61-67 K-cal/mol. The data in Table II even with the degree of scatter between test methods, are all two and a half to five times this value, indicating that the rate controlling process for deformation does not involve self diffusion.

E. Structural Observations

Light Microscopy

Tensile specimens of recrystallized TD Nickel that had been strained various amounts at 2000°F were examined by optical microscopy. The recrystallized structure was produced by rolling as-extruded material 51% in the longitudinal direction and annealing one hour at 2400°F. Specimens strained in the rolling direction showed no internal cracking or fissures at strains of 0.2 to 0.6% offset although some grain boundary cracking was found in fractured specimens. Specimens which were tested at 60° to the rolling direction showed grain boundary cracking at the 0.2% yield strain, Figure 19. Specimens tested transverse to the rolling direction failed before the yield strain was reached, approximately 0.1% offset. These specimens also showed cracking in the gage section away from the fracture, Figure 19. Grain boundary cracking was found at very low strains for all specimens which contained grain boundaries at an angle to the applied stress.

Specimens of as-extruded material which had been tensile tested at 2000°F at various strain rates were also examined by light microscopy. The generalized cracking found after testing, Figure 4,

was found to decrease with increasing strain rates. Specimens tested at .002 crosshead speed had extensive cracking throughout the gage section, at .02 crosshead speed there was less and at .2 crosshead speed almost none. The reduction in area increased sharply with strain rate, Table 10. These observations are consistent with the presence of grain boundary sliding leading to intercrystalline cracking, a process facilitated by low strain rates.

Observations of the electropolished surface of recrystallized specimens strained to the .2YS at 2000°F were made to ascertain if grain boundary sliding was operative. Up to the .2YS there were only isolated displacements of the reference scratches for specimen strained in the longitudinal direction but specimens oriented 60° to the rolling direction showed many instances of sliding at various points. An example is illustrated in Figure 20. For specimens strained to .4% YS isolated sliding was observed for the longitudinal orientation but not nearly as much as the 60° orientation at .2YS.

DISCUSSION

The strength of a dispersion hardened alloy is usually discussed in terms of individual contributions from the particles and the as-worked structure. There is a general feeling that the as-worked structure portion is due to the effects of what is called "cold work". A common explanation for the strength of dispersion hardened alloys is that a large amount of "cold work" or "stored energy" is built up in these materials. The present data have illustrated that the term "cold work" is too nebulous to explain the effects of mechanical working on strength. It has been clearly shown that room temperature and elevated temperature strengths are influenced by different variables. As-extruded and commercial bar have similar strengths at room temperature but differ widely at elevated temperatures. Commercial bar and recrystallized materials have different room temperature strengths but are relatively close in elevated temperature strength. The activation energies and fracture characteristics are also different at high and low temperatures. The present data suggest that only room temperature properties are influenced by cold working or strain hardening. The strength follows the room temperature hardness and, presumably, the dislocation density of the various materials. However, the elevated temperature strength does not correlate with the amount of deformation.

The changes in elevated temperature strength of TD Nickel with mechanical working and recrystallization may be understood by considering the role of grain boundaries during deformation. The

proposed source of low strength in various TD Nickel structures is the premature failure of grain boundaries inclined at some angle to the stress axis. It then follows that structures which contain grain boundaries parallel to the applied stress are strong. Data supporting this viewpoint will be presented for the fully recrystallized material and comparison made with results of nickel-base superalloys which have been directionally solidified to a columnar grain structure. Evidence for considering the strength of fine grained as-extruded and commercial bar material to be controlled by grain boundaries will be presented next and, finally, the mechanism of grain boundary failure will be briefly discussed.

It is known that the directional solidification of a nominally brittle Ni-Cr-Al alloy results in increased rupture life and ductility in the longitudinal direction (21). Testing the columnar structure at various angles from the longitudinal direction reduced both rupture life and ductility. The fracture was intergranular and the fracture surface followed the grain direction in all cases. The reason for the increased rupture life is that rupture is controlled by intercrystalline fracture which, at elevated temperatures, is initiated at grain boundaries. The orientation of the grain boundaries out of parallel to the direction of the applied stress caused early failure during the test and reduced life. It is for this reason that a coarse grain size with few transverse boundaries is preferred in nickel base superalloys. Similar increases in strength and ductility with directional solidification have been

produced in other nickel base superalloys, including Mar-M200, B-1900, IN-100 and TRW 1900 (22).

The grain shape of recrystallized TD Nickel produced by rolling and annealing is analogous to the grain shape of unidirectionality solidified nickel base superalloys. The TD Nickel structure has a coarse transverse grain dimension and an appreciable length dimension, the width to length ratio being approximately 1:20. The majority of the grain boundaries are aligned in the longitudinal direction. As with the columnar superalloy, the strength and ductility of recrystallized TD Nickel are a maximum in the longitudinal direction. The fracture locus in tensile testing TD Nickel is the grain boundary as shown in Figure 14. The brittleness of the material when loaded at right angles to the grain boundaries is indicated by the load-deflection curve of Figure 12. Even though the longitudinal test specimens displayed high elongation and reduction in area, indicating that individual grains are ductile, the transverse tests revealed that a brittle type of failure is produced by failure of the grain boundaries. The ductile nature of specimens pulled along the grain boundaries compared to the brittle behavior of specimens containing grains at an angle is clearly shown in Figure 14.

The localized failure which occurs within grain boundaries was convincingly demonstrated by the micrographs of Figure 19. Figure 19 shows grain boundary cracking at very low strains for the specimen axis skewed to the loading axis. The presence of grain

boundary sliding was also found only for specimens taken at orientations other than longitudinal.

Since a columnar grain structure produces strength and ductility in the longitudinal direction, the variation in tensile strength with rolling direction may be understood in terms of the recrystallized grain shapes produced. The recrystallized grains obtained after prior transverse rolling are not as elongated as the grains obtained after prior longitudinal rolling, Figure 14. Hence, with more grains inclined to the stress axis the strength and ductility are lowered.

The low strength of as-extruded material and transverse specimens of commercial bar may also be considered in terms of grain boundary failure. Several factors suggest that the behavior of these fine grained materials is the same as recrystallized material. One factor is the high activation energy which the coarse and fine grain materials have in common. Both materials also have intercrystalline fractures. The fracture surfaces and the orientation of internal cracking also indicate that failure always occurs across the grain direction. Support for the concept of grain boundaries failing early in the tensile process is provided by the apparent lowering of the modulus for the low strength materials and orientation. Such a lowering is probably due to small amounts of internal cracking.

Previous work has demonstrated that grain boundary sliding is active in commercial TD Nickel bar (12), and grain boundary

sliding with eventual fracture has been proposed to account for the lowering of ductility with increasing test temperature in dispersion hardened alloys. Indirect evidence for the presence of grain boundary sliding in the present work is provided by the increase in ductility with strain rate in Table 10, an effect normally associated with grain boundary failure.

To explain the results of the present study in terms of grain boundary failure; the as-extruded material is in a relatively weak condition because a large number of grain boundaries exist at various angles to the applied stress, Figure 1. Because of this general low strength level, there is no great directionality in strength although the transverse strength is slightly lower. Swaging produces a fibered grain structure which is strong in the longitudinal direction but still weak in the transverse direction. Recrystallization will also increase the longitudinal strength of as-extruded material both by producing aligned grain boundaries and by increasing the grain size which reduces the overall grain boundary area. The relatively high transverse strength of the recrystallized material is due to the increased grain size which exposes a smaller grain boundary area to tensile stress. The effect of torsion on strength is to incline grain boundaries at an angle to the axis. The loss of strength with upsetting is due to buckling and twisting of grains with upset deformation.

Although the point has not been conclusively proven in the present study, it appears that total dislocation density is not a

major factor in elevated temperature strengthening. This conclusion is based on the high strength of the recrystallized structure. The elevated temperature strength was also insensitive to annealing at temperatures up to 2500°F. However changes in room temperature strength and hardness suggest that the dislocation density was lowered. Finally, the cold swaging of the recrystallized structure did not produce appreciable elevated temperature strengthening.

The ductility observations may also be explained by grain boundary failure. The ductility of the recrystallized material is very much like a directionally solidified nickel base superalloy, ductile in the longitudinal direction but brittle in the transverse. The true ductility in the low strength condition of as-extruded or commercial bar materials is probably low, but internal cracking leads to a high measured value. The differences in measured ductility of coarse and fine grained materials is most likely due to the differences in fracture path.

While the failure process in elevated temperature tensile testing has been attributed to grain boundary failure and the strength changes have correlated with the orientation of grain boundaries to the stress axis, it has not been possible to follow the precise sequence of grain boundary failure. Much more detailed study by both replica and transmission electron microscopy will be required to follow the fine details of the process. However, it has been established that the grain boundary is the locus of failure in TD Nickel tensile fracture and that grain boundary sliding is

operative. It is known that intercrystalline cracking is frequently produced by the grain boundary sliding and that, if the intrinsic internal strength of the alloy grains are high, that failure is almost completely by intergranular cracking. It is also known that the tendency for cracking may be reduced by migration of the grain boundary. The most likely failure process in TD Nickel is then a sequence of grain boundary sliding with the early production of intercrystalline cracking. Because of the pinning effect of thoria on grain boundaries, no migration is possible and the cracking process continues until fracture. High strength in dispersion hardened alloys is then possible only with a structure which does not fail prematurely in the grain boundary; i.e. a structure with boundaries parallel to the applied stress. Any comparison of secondary variables which influence elevated temperature strength, such as interparticle spacing, must be performed with a common grain structure.

The presence of thoria particles in the nickel matrix serves two functions, internal strengthening of the grain and retarding boundary movement. The internal strengthening is most likely due to direct particle interaction with dislocations rather than indirect interaction via dislocation tangles. The retardation of grain boundary movement results in the stabilization of the specific grain morphology produced by mechanical working. It has been shown that the combined presence of thoria particles and a fibered grain shape will produce excellent elevated temperature properties. However, if grain boundaries were loaded in shear, failure occurred at very low stresses. These results indicate that, even with the thoria addition, the grain boundary strength is lower than the strength within the grain. Utilization of the strengthening effect of thoria particles was found only when premature grain boundary failure was avoided through prior alignment of grain boundaries by mechanical working.

RECRYSTALLIZATION BEHAVIOR

INTRODUCTION

The effect of a finely dispersed hard particle second phase on recrystallization has been the subject of investigations on both single and polycrystalline materials, and the results have been summarized by several authors (23,24). It is generally found that a finely dispersed phase will retard recrystallization although some exceptions have been noted. The recrystallization resistance is usually considered in terms of the particles interfering with normal nucleation and/or growth processes. The work of Brimhall and Huggins (25) on internally oxidized silver and aluminum alloys is of special interest because it points out that the as-worked dispersion hardened structure is different than the pure matrix given comparable deformation. This observation suggests that the particles may play an active role in the development of a recrystallization resistant structure rather than the more passive role of generally resisting boundary movement. It is the purpose of the present study to illustrate that recrystallization resistance in a commercial dispersion hardened alloy, TD Nickel, requires not only the presence of the dispersed phase but also a particular prior deformation history.

TD Nickel, a DuPont product containing two volume percent thoria in a nickel matrix, is a commercial dispersion hardened alloy useful for high temperature applications. Although the as-received cold worked bar will not recrystallize after one hour at 2500°F (5),

various subsequent working operations may produce one-hour-recrystallization temperatures ranging from 840°F (almost the same as pure nickel) to above 2500°F (5,20,26) for comparable percent reductions. The specific cold working operation employed appears to exert a strong influence on recrystallization behavior; in one instance cold swaging up to 75% did not lead to recrystallization while cold rolling reductions as low as 35% would recrystallize (5). Similar differences between swaging and rolling have been found for nickel thoria alloys produced by mechanical mixing (27). The present study has examined the influence of working operation, working direction, and reduction upon the recrystallization behavior of TD Nickel in an attempt to define the factors which control the recrystallization process.

EXPERIMENTAL PROCEDURE

The materials used were previously described in the MATERIALS section. Neither the as-extruded nor the commercial TD Nickel bar would recrystallize after one hour at 2400°F.

The cold working operations selected for the program were swaging and rolling. Samples of as-extruded material to be swaged were prepared by slitting a length of the extrusion into quarters and machining the quarters to one inch diameter. As-extruded and one inch commercial bars were then both cold swaged in passes of 15% to a total reduction of 95% with lengths cut off at intermediate reductions. No intermediate stress reliefs were employed and neither bar showed a tendency for cracking during swaging.

Rolling samples were sectioned to a common width from areas indicated in Figures 21 and 22. The faces were machined parallel to .250" thickness, and the surfaces ground on 240 grit metallographic paper. The rolling directions referred to as longitudinal, transverse, and radial, have reference to the extrusion or bar axis. Longitudinal and transverse pieces were cold rolled through a 10" mill with the same side up and the same end into the rolls on each pass. The radial pieces had the same side up but were rotated 90° clockwise each pass. Reductions were approximately 20% per pass with lubrication being used only above 80% total reduction. A single sample was rolled to each reduction evaluated. No intermediate stress relief treatments were used and severe cracking was encountered for the as-extruded material at total reductions in

excess of 60%. The commercial bar stock rolled in the transverse direction exhibited some slight cracking above 80% reduction. In all cases sufficient sound material was available for evaluation.

Metallographic sections of a plane normal to the rolled surface containing an axis parallel to the original bar or extrusion direction were cut from the center of each sample, and heat treated in a platinum wound tube furnace controlled to $\pm$ 5°F in an atmosphere of flowing argon. Because coarsening of thoria has been reported in TD Nickel above 2450°F (20), 2400°F was the highest recrystallization temperature employed. The percent recrystallization was measured with a planimeter for representative micrographs. Rockwell G hardness readings were taken on the swaged samples and microhardness readings taken on sheet specimens. Reported microhardness readings are the average of measurements of both diagonals taken on at least 5 Vickers impressions located at the center line of the sheet thickness.

Specimens were prepared for texture determination by grinding to the center of the sheet thickness, metallographically polishing through Linde A abrasive, and electropolishing in a 10% H_2SO_4-90% methanol solution. Texture at the rolled surface was measured after a light electropolish. Pole figures were obtained in reflection with a Norelco pole figure device using copper K_α radiation. The specimen area irradiated was approximately .040"x .040". With receiving slits removed, defocusing losses were less than 10% out to 70° so no correction was applied.

RESULTS

The micrograph shown in Figure 11 illustrates a structure typical of all partially recrystallized samples. The recrystallized grains were characterized by a relatively large (.05 mm x 1mm) grain size and were elongated in the initial bar or extrusion direction regardless of the direction of secondary working. The fine twin structure previously reported for this material (5,6,26) is contained within the recrystallized grains. The dark areas are regions of unrecrystallized material in which the one micron grain size cannot be resolved. The room temperature strength and hardness of this structure, tabulated in Table 12, are much lower than for the two starting materials.

The degree of recrystallization after various one hour annealing temperatures is summarized in Tables 13 and 14 for the various reductions and working operations. The percent recrystallization was measured at the central portion of the sheet thickness but, except where noted, was approximately the same throughout the specimen. No recrystallization was found for any swaging reduction after a 2400^{o}F anneal, verifying previous observations that swaging reductions do not favor recrystallization (5). The presence of recrystallization after rolling depended both upon the rolling direction and the starting material. The influence of rolling direction is evidenced most strongly for commercial bar where specimens rolled in longitudinal passes would not recrystallize, while specimens rolled in transverse passes would recrystallize as

low as 1250°F. A similar trend may be present for the as-extruded material but the differences here are very slight. The commercial bar material would recrystallize only after large reductions when rolled in the radial direction. Of the two different starting materials, the as-extruded material appeared more prone to recrystallize.

An unusual effect is found after large reductions of the as-extruded materials. Whereas small reductions led to extensive recrystallization, the very large rolling reductions served to prevent recrystallization. This retardation, which was noted to some extent for all three rolling directions of as-extruded material, always started at the sheet surface. Typical behavior is illustrated in Figure 23 which shows the development of a recrystallization resistant structure. Just the reverse effect was noted in the radial passes of commercial bar. In this case, deformation of a recrystallization resistant structure finally produced recrystallization which started at the specimen surface. Specimens exhibiting a surface effect are noted in Tables 13 and 14 in brackets indicating the percent recrystallization at the center, surface, and the overall average.

Room temperature hardness values for both rolled and swaged specimens increased with increasing percent deformation, up to the maximum reductions employed, even for the samples which became resistant to recrystallization. No differences in as-rolled hardness either between the hardness values for different rolling directions at a constant reduction or differences between sheet

center and surface, were found to account for differences in recrystallization temperature. The hardness after annealing correlated with the amount of recrystallization with a fully recrystallized structure having a hardness of 190-210 VHN and a partially recrystallized structure having a hardness of 230-210 VHN. The change in recrystallization temperature with rolling direction for commercial bar is reflected in the hardness plots of Figure 24. The sharp drop in hardness at 1250°F for the transverse rolling direction is due to recrystallization. Of the remaining data points in this figure, recrystallization was found only for the sample rolled in the radial direction and annealed at 2400°F. The retardation of recrystallization with increasing rolling reductions is illustrated in Figure 25 for as-extruded material. Material rolled 59% in the longitudinal direction was almost completely recrystallized after one hour at 2400°F while material rolled 90% reduction in the same direction would not recrystallize. In like manner, material rolled only 57% in radial passes was almost completely recrystallized while specimens rolled to 90% reduction were only partially recrystallized.

Crystallographic textures of all rolled and swaged samples were determined using a standard reflection method. The initial fiber texture of the two starting materials is shown in Figures 26 and 27. The commercial bar had a strong, almost perfect, duplex texture consisting of [200] and [111] components with the half width of the central (200) or (111) line approximately 6°. The

as-extruded material had a much weaker texture also containing [200] and [111] components and a wide central half peak width of about 22°.

The texture changes which accompany the development of a recrystallization resistant structure in longitudinal rolling of as-extruded material are shown in Figures 28-30. At 37% a mild rolling texture has developed; at 74% the texture has become more pronounced and at 90% still further sharpening has occurred. The texture shown in Figure 30 is common to rolling directions which displayed resistance to recrystallization, i.e. the longitudinal passes of commercial bar, Figure 31, and to a lesser degree the transverse passes of as-extruded material, Figure 32. The texture is not composed of a single ideal texture but may be approximated by a combination of (123) [412] and (146) [211] . In samples containing an unrecrystallized surface layer, especially the longitudinal as-extruded passes, the texture at the surface was closer to Figure 30 than was the center.

The extreme difference in recrystallization behavior between longitudinal and transverse rolling of commercial bar is accompanied by a difference in as-rolled texture. The texture after transverse rolling is close to an ideal (100) [010] , Figure 33, and is not as sharp as the longitudinal texture.

The textures developed by radial rolling are difficult to analyze, probably a result of the cross flow taking place upon successive 90° rotations. The commercial bar had an initial strong

fiber texture but successive rolling passes tended to destroy this. The texture changed at the surface before the center of the specimen. Recrystallization also was initiated at the specimen surface in this series.

The fiber textures found after various swaging reductions are listed in Table 15. Specimens were placed in the pole figure unit and aligned to reach maximum intensity in the fiber direction. A ϕ scan of the central peak was then made and the maximum intensity and peak half width are listed in Table 15. The relative proportion of (111) to (100) texture is listed in Table 15. The texture sharpens appreciably from the as-extruded condition particularly at the lower reductions. The mixed [11] [00] fiber components persist throughout the deformation history although the (111) increases with greater reductions.

DISCUSSION

The unique feature of the recrystallization behavior of TD Nickel is the relative insensitivity of the percent recrystallized to the percent of deformation. This effect is most pronounced for as-extruded samples rolled in the longitudinal direction where the specimens given larger reductions would not recrystallize even though the specimens given lower reductions recrystallized extensively. The trend is also noted in the extruded-transverse and extruded-radial sequences. The amount of recrystallization does not follow the amount of strain hardening since the room temperature hardness of all sequences increased with increasing percent reduction. The deformation process has evidently produced a structure that is resistant to recrystallization in spite of a high degree of strain hardening. The swaging process seems particularly effective in producing this recrystallization resistant structure. The stabilization of structure is due completely to the deformation since no intermediate anneals were employed.

A potential mechanism for the retardation of recrystallization with mechanical working may involve the as-worked crystallographic texture. Variation in recrystallization temperatures with the texture of the as-deformed material has been frequently reported for single crystals. For example, single crystals of copper and aluminum may be heavily deformed without change in their initial crystallographic orientation and recrystallization takes place with great difficulty in such crystals (29,30). Recrystal-

lization temperatures also vary with deformation texture in cold rolled silicon iron crystals (31,32) and in copper single crystals (32). These single crystal results have been reviewed recently by Hu (33). Deformation texture is also reported to affect recrystallization temperature and kinetics in polycrystals, copper (34,35) and iron (36) being two examples. The mechanism for the variation is not completely clear but has been discussed in terms of the specific texture produced (33) or the sharpness of the deformation texture (37).

Since texture so obviously influences the recrystallization temperature of single crystals, the lack of more extensive data on polycrystalline materials is an obvious question. The probable reason for the lack of data is that in a random polycrystalline material, many grains are oriented for easy recrystallization and the texture retardation is not produced until a highly perfect texture has been obtained. In the case of copper (34,35) and iron (36), deformations of 96-99% were employed to achieve a high degree of texture. In commercial TD Nickel bar, a high degree of texture is present in the starting material because of the prior processing history and lack of recrystallization anneal. Any influence of texture on recrystallization would then be noted at lower reductions.

Fcc rolling textures are of two general types usually called copper type and brass type or sometimes pure metal type and alloy type. The copper type, while characteristic, is difficult to

define in terms of a single ideal orientation but may be approximated by (123) $[41\bar{2}]$ or (123) $[41\bar{2}]$ + (146) $[211]$ (37). The brass type is close to a (110) $[1\bar{1}2]$ but sometimes contains a (110) $[00\bar{1}]$ minor component. Pure nickel sheet textures are of the copper type (39,40). The texture of cold rolled nickel-$2\frac{1}{2}$% thoria has also been reported as copper type (40,27) but the ideal orientation in the latter investigation was (135) $[11\bar{2}]$ which is just slightly off the usual designations for a copper type texture. The addition of thoria is reported to produce a more pronounced texture at a given reduction than pure nickel (40). The thoria also tended to stabilize any prior texture with rolling reductions in excess of 90% required to eliminate the previous pattern (27). TD Nickel rolled in longitudinal and transverse passes had a (110) $[00\bar{1}]$ texture (20).

In the present study, the as-rolled sheet texture of samples which did not recrystallize are of the copper type. These samples include the longitudinal passes of commercial bar, Figure 31, and longitudinal and transverse passes of as-extruded material, Figures 30 and 32. The surface of as-extruded specimens rolled in the longitudinal direction did not recrystallize. The texture of the surface is closer to the copper type texture than the texture of the center, where recrystallization occurred. Note that the transition from the fiber texture to the sheet texture requires a minimum texture change for the commercial bar, as indicated by comparison of Figures 26 and 31. During these rolling passes

recrystallization could not be produced. Conversely, the initial texture of the as-extruded material is weak and considerable readjustment is necessary to reach the final texture. These specimens recrystallized readily at the low rolling reductions. The sample which had the lowest recrystallization temperature came from the transverse rolling of commercial bar stock. This texture was a relatively weak (100) [010] .

Fcc metals have duplex fiber texture composed of [111] and [100] components. In pure nickel the [100] component is found only at low reductions while the [111] component predominates at higher deformation. The reported percentage of [111] has been reported from 83 to 100% (41,27,42). In a nickel thoria alloy, the [100] component is not as easily supressed, being reported at 60% after a 95% cold drawing reduction (27). However, the percentage of [111] does increase with the degree of working. This stabilization of an intermediate textured component is similar to results for rolling. It has been suggested (43) that processes which interfere with cross slip will stabilize the [100] texture. However, it has not been established that the dispersed particles inhibit cross slip. The theory is also in disagreement with the observation of a [100] fiber texture in aluminum, a material in which cross slip should occur readily (44).

The texture of TD Nickel bar has been reported as primarily [100] (45,20,12). The present work shows a mixed [111] and [100] texture for the commercial bar with an increase in [111] with deformation.

The [100] component has been reported to increase slightly with annealing (27,40). The difference in texture between the present study and previous data may be due partially to measuring the as-deformed texture. It is also possible that the present lot of material was worked more which would also increase the [111] component.

The inhibition of nucleation is the generally acknowledged mechanism for the retardation of recrystallization (23) by a dispersed phase. The very coarse recrystallized grain size reported for SAP (46) and TD Nickel (20) and the grain size found in the present study are consistent with this observation. The dispersed particles do appear to influence growth, as evidenced by the elongated recrystallized grain shape. Similar grain shapes are observed in SAP (46) and in tungsten wire.

Two current theories of nucleation are the bulge theory by Bailey and Hirsch (47) and the growth or coalescence of sub-grains advanced by Li (48) and Hu (33). The bulge theory treats the localized bulging of a grain boundary from a region of low dislocation density to a region of high dislocation density. This mechanism suggests that nucleation is really an early stage of growth. Evidence for the operation of the bulge theory has been reported for moderately deformed nickel (47). The growth or coalescence of sub-grains treats the production of nuclei from the movement of low angle subgrain boundaries either with or without subgrain rotation. This mechanism has also been reported in

nickel (49).

The retardation of nucleation by the production of a sharp texture is consistent with either theory. The bulge theory requires the movement of high angle grain boundaries. However, the presence of a strong single component texture has been reported to reduce the mobility of grain boundaries by a process called texture stabilization - (50) or texture inhibited growth - (51). The decrease in mobility has been discussed more fully by Dunn and Walter (52). While the effect is a growth process occurring during secondary recrystallization, it should also apply to growth to localized bulging. Evidence in the literature also indicates that texture may influence the low angle grain boundary movement either through mobility or driving force. For example, the rate of polygonization in aluminum(53) and copper crystals (54) has been shown to depend upon the as-worked crystal orientation. The relative orientation of sub-grains, which is reflected in a texture measurement, also influences the driving force of low angle boundary movement. As an example of the latter case, rolling of single crystal silicon iron crystals in a direction to maintain an initial (001) [110] orientation produced a sharp texture, a uniform substructure, and a high recrystallization temperature. Cross rolling to produce a (001) [210] orientation resulted in a non-uniform substructure, misorientation between sub-grains, and low recrystallization temperature (31). The retardation of recrystallization by a sharp texture could be due to either high angle or low angle boundary effects.

CONCLUSIONS

1. There is no correlation between room and elevated temperature strength of TD Nickel. The strength is controlled by different processes at room and elevated temperatures with the room temperature tensile properties being "normal" in response to mechanical working and annealing.

2. Cold swaging deformations produce strengthening at both room and elevated temperatures.

3. Upset forging and prior room temperature torsion lower the elevated temperature strength.

4. A fully recrystallized structure has very high strength at elevated temperatures but low strength at room temperature compared to the fine grained cold worked starting material.

5. High activation energies, $2\frac{1}{2}$ - 5 times nickel self-diffusion, were found in tensile testing of as-extruded, commercial bar, and recrystallized structures.

6. Recrystallized TD Nickel fails by intercrystalline cracking. The failure process, which occurs at very low strains if grain boundaries are not parallel to the applied stress, constitutes a serious limitation on strength.

7. The data on fine grained TD Nickel indicate that these materials also fail by grain boundary failure.

8. It is concluded that the presence of grain boundaries parallel to the applied stress is a necessary condition for elevated temperature strengthening in dispersion hardened alloys.

9. Additional strengthening through the presence of a dislocation substructure or finer interparticle spacing will be effective only if premature grain boundary failure is avoided.

10. Recrystallization in TD Nickel is influenced more by the specific working operation and working direction than the degree of strain hardening.

11. Recrystallization could not be obtained after swaging reductions of 15 - 95%.

12. Recrystallization for a given rolling reduction varied with the rolling direction.

13. Continued rolling deformation in one direction produced a more recrystallization resistant structure in spite of increased strain hardening.

14. A structure resistant to recrystallization always had a sharp crystallographic texture.

15. The presence of a sharp texture is consistent with the inhibition of nucleation by either of the two current nucleation theories.

REFERENCES

1. A. Kelly and R. B. Nicholson, Progress in Materials Science, 10 no. 3 (1963).

2. G. S. Ansell, Oxide Dispersion Strengthening, Gordon and Breach, (1966).

3. R. W. Guard in Strengthening Mechanisms in Solids, Reinhold, (1962).

4. N. J. Grant in Strengthening of Metals, Reinhold, (1964).

5. G. S. Doble and R. J. Quigg, Trans. AIME 233, 410 (1965).

6. M. C. Inman, K. M. Zwilsky and D. H. Boone, ASM Trans. Quart. 57 701 (1964).

7. L. J. Klingler and D. B. Arnold, Oxide Dispersion Strengthening, Gordon and Breach, (1966).

8. G. S. Ansell and F. V. Lenel, Trans. AIME 221 452 (1961).

9. G. S. Ansell and J. Weertman, Trans. AIME 215 838 (1959).

10. C. L. Meyers and O. D. Sherby, J.Inst. of Metals, 90 380 (1961-62).

11. B. A. Wilcox, Oxide Dispersion Strengthening, Gordon and Breach, (1966).

12. B. A. Wilcox and A. H. Clauer Trans. AIME 236 570 (1966).

13. C. I. Bradford, Steel , Oct. 31, 1966.

14. H. Conrad, Mechanical Behavior of Materials at Elevated Temperatures, McGraw-Hill, (1961).

15. C. Susse, J. de Phys., 17 910 (1956).

16. Z. S. Basinski, Acta Met., 5 684 (1957).

17. N. J. Grant, Mechanical Behavior of Materials at Elevated Temperatures, McGraw-Hill, (1961).

18. H. W. Swift, J. Iron and Steel Inst., 140 181 (1939).

19. W. A. Backofen and B. B. Hundy, J. Inst. Met., 81 433 (1952-3).

20. M. C. Inman and P. J. Smith, Oxide Dispersion Strengthening, (1966).

21. F. L. Ver Snyder and R. W. Guard, Trans ASM 52 (1960) 485.

22. B. J. Piearcey and B. E. Terkelsen, Trans AIME 239 (1967) 1143.

23. R. W. Cahn, Recrystallization, Grain Growth and Textures, ASM, 99 (1966).

24. J. L. Brimhall, M. J. Klein, and R. A. Huggins, Acta Met., 14 459 (1966).

25. J. L. Brimhall and R. A. Huggins, Trans. AIME, 233 1076 (1965).

26. M. Von Heimendahl and G. Thomas, Trans. AIME, 230 1520 (1964).

27. P. B. Mee and R. A. Sinclair, J. Inst. of Met., 94 319 (1966).

28. P. Guyot, Mem. Sci. Rev. Met., 61 555 (1964).

29. Y. C. Liu and W. R. Hibbard, Jr. Trans. AIME, 197 672 (1953).

30. A. H. Lutts and P. A. Beck, Trans. AIME, 200 257 (1954).

31. C. G. Dunn and P. K. Koh, Trans. AIME, 206 1017 (1956).

32. W. R. Hibbard,Jr. and W. R. Tully, Trans. AIME, 221 336 (1961).

33. Hsun Hu in Recovery and Recrystallization of Metals p. 311 Interscience (1963).

34. R. M. Brick and M. A. Williamson, Trans. AIME, 143 84 (1941).

35. J. R. Michalak and W. R. Hibbard,Jr., Trans. AIME, 209 101 (1957).

36. J. T. Michalak and W. R. Hibbard,Jr., Trans. ASM, 53 331 (1961).

37. C. S. Barrett and T. B. Massalski, Structure of Metals, McGraw-Hill, 556 (1966).

38. C. G. Dunn and P. K. Koh, Trans. AIME, 206 1017 (1956).

39. K. Detert, P. Dorsch and H. Migge, Z. Metal, 54 263 (1963).

40. C. A. Clark and P. B. Mee, Z. Metal., 53 756 (1962).

41. H. Ahlborn and G. Wassermann, Z. Metal., 53 423 (1962).

42. P. Dayal and R. Sharan, Eastern Metals Rev., 14 117 (1961).

43. N. Brown, Trans. AIME, 221 236 (1961).

44. K. S. Sree Harsha and B. D. Cullity, Trans. AIME, 224 1189 (1962).

45. R. K. Ham and M. L. Wayman, Trans. AIME, 239 721 (1967).

46. E. J. Westerman and F. V. Lenel, Trans. AIME, 218 1010(1960).

47. J. E. Bailey and P. B. Hirsch, Proc. Roy. Soc. 267A 11(1962).

48. J.C.M. Li, JA Phys. 33 2958 (1962).

49. W. Bollman, J. Inst. Met. 87 439 (1959).

50. P. A. Beck, Trans. AIME, 185 311 (1949).

51. K. T. Aust, The Art and Science of Growing Crystals, Wiley, p. 452, (1963).

52. C. G. Dunn and J. L. Walter, Recrystallization, Grain Growth and Textures, ASM, p.461, (1965).

53. W. G. Burgers, Y. H. Liu and T. J. Tiedema, Proc.Kon. Ned. Acad., v Wet, 54 459 (1951) quoted by Beck and Hu, Recrystallization, Grain Growth and Textures, ASM p.402 (1965).

54. C. T. Wei, M. N. Parthasarathi and P. A. Beck, J. App. Phys. 28 874 (1957).

TABLE 1

VENDORS CHEMICAL ANALYSIS OF TD NICKEL LOT 2294

ELEMENT	%
C	.0038
Ti	<.001
Fe	.002
Cr	<.001
Co	.01
Cu	.003
S	.002
ThO_2	2.4

TABLE 2

BASE LINE TENSILE PROPERTIES

Material Condition	Yield Strength(psi) 0.2%Offset	Ultimate Tensile Strength(psi)	Red.in Area%	%Elongation
		ROOM TEMPERATURE		
commercial bar-L	90,600	101,800	83	14.6
commercial bar T	83,600	97,400	35.5	12
as-extruded L	92,100	105,000	66.5	13.4
as-extruded T	90,000	103,800	23	9.7
		2000°F		
commercial bar-L	14,700	17,900	1	4.4
	12,400	17,600	7	*
commercial bar 45° to bar axis	4,350	5,340	24	33
	3,160	4,290	30	35
commercial bar-T	2,800	3,500	11.8	15.5
	2,550	3,350	12	12.4
as-extruded-L	3,840	4,160	26.5	20.5
	3,850	4,250	18.3	16
as-extruded-T	3,240	3,540	15.1	*
	3,240	3,690	12	14.5

* = specimen damaged and could not measure
specimen gage = .080" x .400"
crosshead speed = .005"/min

TABLE 3

EFFECT OF ELEVATED TEMPERATURE EXPOSURE ON TENSILE PROPERTIES

Material Condition	Yield Strength(psi) 0.2% Offset	Ultimate Tensile Strength(psi)	Red.in Area%	%Elongation
		2000°F		
commercial bar	18,650	19,000	9	4.8
	18,700	19,300	5.3	8.3
commercial bar +1/2300°F	17,300	18,100	3	2.6
commercial bar +1/2500°F	18,700	19,000	5	1.1
as-extruded*	3,840	4,160	26.5	20.5
	3,850	4,250	18.3	16
as-extruded +1/2300°F	3,400	3,760	40	19.5
		ROOM TEMPERATURE		
	Prop. Limit			
commercial bar	42,000 85,500	104,500	61	11.4
	40,500 86,000	105,000	63	12.5
commercial bar +1/2300°F	77,000	95,600	84	19
	78,100	95,500	85	18.7
commercial bar +1/2500°F	74,900	92,600	84	17.6
as-extruded	49,000 88,400	103,200	83	11.5
	50,700 89,000	104,000	80	11

TABLE 3 (continued)

as-extruded +1/2300°F	83,000	97,600	72	18.5
	83,000	97,600	74	17.8

* .080" x .400" gage section and .005"/min crosshead
specimen gage = 160" x 1.25"
crosshead speed = .020"/min

TABLE 4

EFFECT OF COLD SWAGING ON 2000°F TENSILE PROPERTIES OF AS-EXTRUDED TD NICKEL

Swaging Reduction(%)	Yield Strength(psi) 0.2% Offset	Ultimate Tensile Strenght(psi)	Red.in Area %	% Elong.
0	3,840	4,160	26.5	20.5
	3,850	4,250	18	16
26	5,070	5,760	9.7	*
	5,240	5,950	8.5	11.5
45	6,100	6,840	17	15.5
59	7,450	9,400	17	8.1
75	7,500	14,000	4.6	5.2
82	16,700	18,100	6	4.2
	15,500	18,300	3.6	2.2
90	15,600	19,000	1.2	*
95	17,900	19,200	7.3	4.2

* specimen damaged and could not measure
specimen gage = .080" x .400"
crosshead speed = .005"/min

TABLE 5

EFFECT OF COLD SWAGING ON 2000°F TENSILE PROPERTIES OF 1" COMMERCIAL TD NICKEL BAR

Swaging Reduction (%)	Yield Strength(psi) 0.2%Offset	Ultimate Tensile Strength(psi)	Red.in Area%	%Elongation
0	18,650	19,000	5.9	4.8
	18,700	19,300	5.3	8.3
59	19,400	22,000	1	*
75	20,900	24,100	1.6	2.6
84	24,000	25,400	6	2.8
90	22,600	24,600	3	.5
95	23,000	25,000	3	5

* specimen damaged and could not measure

specimen gage .113" x1.25"

crosshead speed = .020" / min

TABLE 6

EFFECT OF UPSET FORGING ON 2000°F TENSILE PROPERTIES OF 1" COMMERCIAL TD NICKEL BAR

Material Condition		Yield Strength(psi) 0.2% Offset	Ultimate Tensile Strength(psi)	Red.in Area %	% Elong.
commercial 1" bar	L	14,700	17,900	1	4.4
		12,400	17,600	3.2	*
	T	2,800	3,500	11.8	15.5
		2,550	3,350	12	12.4
upset 15% RT	L	14,000	15,200	8	6.7
		11,600	14,200	5	5.5
	T	2,250	3,380	12.5	*
		2,500	3,280	9.8	*
upset 35% RT	L	6,100	7,610	18.5	11.5
		5,960	7,660	24.6	11
	T	3,100	3,880	8.5	16
		2,950	3,930	10.8	17.5
upset 50% RT	L	3,930	4,720	20	12
		4,270	5,160	16.7	11.5
Edge -	L	5,110	6,300	15.6	14.5
		5,620	7,300	12.1	13.5
	T	3,080	3,880	21.3	13.6
		3,080	3,880	21	16.5
upset 50% 1000°F	L	4,280	5,260	10	12.5
		3,980	5,170	16.7	*
	T	3,730	4,220	10.8	*
		3,630	4.030	10.9	*

TABLE 6 (continued)

upset 50% 1500°F	L	3,580	4,870	16.5	14
		3,630	4,930	17	15
	T	3,170	4,190	12.2	10
		3,730	4,020	14.5	10
upset 50% 2000°F	L	3,050	3,640	15.5	13
	T	3,150	3,640	13	10
		3,340	3,640	9.5	8.6

* specimen damaged and could not measure
specimen gage .080" x .400"
crosshead speed .005"/min

TABLE 7

EFFECT OF PRIOR TORSIONAL STRAIN ON 2000°F
TENSILE PROPERTIES OF COMMERCIAL TD NICKEL BAR

Material Condition	Yield Strength (psi) 0.2%Offset	Ultimate Tensile Strength (psi)	Red. in Area%	%Elongation
commercial bar	15,700	18,400	3	4.9
	16,500	17,500	3.4	*
commercial bar twisted 120°	14,300	15,800	2.1	5.7
commercial bar twisted 240°	11,800	13,100	8.2	2.7
commercial bar twisted 120° ± untwisted 120°	15,800	17,600	5	7
	15,500	18,000	6.4	5.5

* specimen damaged and could not measure

gage section .173 x .850"

crosshead speed .010"/min.

TABLE 8

2000°F TENSILE PROPERTIES OF RECRYSTALLIZED TD NICKEL

Material Condition		Yield Strength(psi) 0.2% Offset	Ultimate Tensile Strength(psi)	Red.in Area %	% Elong.
as-extruded + 1/2500°F (50-70% re-crystallized)	L	15,250	15,950	26	9.2
		11,000	11,500	15	3.5
	45°	7,700	7,900	3	2.9
		4,250	4,750	6	4.9
	T	5,400	5,500	3	2.6
		4,500	4,900	4	3
as-extruded + rolled 51% L + 1/2400°F (100% re-crystallized)	L	19,400	20,000	24.7	5.6
		18,800			
	60°	19,150	19,200	3	2.8
	T	**	15,150	0	2
		**	14,100	0	
as-extruded + rolled 50% in L,T or both directions + 1/2400°F all test L to extrusion axis (100% recrystallized)	L (rolling)	18,800	19,500	21.5	7.6
		18,700	19,200	32	6.8
	L&T (rolling)	18,700	19,900	13	6.3
		18,700	19,100	11	4.4
	T (rolling)	17,200	17,300	2	3.6
		16,900	17,100	1.5	1.6

* .113" x .750" gage section and .010"/min crosshead speed

** fractured before reaching yield strain

TABLE 9

EFFECT OF COLD WORK ON 2000°F TENSILE PROPERTIES

OF RECRYSTALLIZED TD NICKEL

Material Condition	Yield Strength(psi) 0.2% Offset	Ultimate Tensile Strength(psi)	Red.in Area %	% Elongation
recrystallized (as-extruded and rolled 47% in longitudinal direction + 1/2400°F)*	19,200	19,600	13	6.6
	18,900	19,500	18.3	5.2
recrystallized + cold swaged 50%	19,700	20,500	15.5	12
	18,900	19,700	25	11

* gage section .113" x 1.25 and .020"/min crosshead speed

** gage section .080" x .400" and .005"/min crosshead speed

TABLE 10

TENSILE PROPERTIES OF TD NICKEL

Test Temp. °F	Speed(in/min.)	Yield Strength(psi) 0.2% Offset	Ultimate Tensile Strength(psi)	Red.in Area %	% Elong.
		as-extruded + 1/2300°F			
1800	.002	4,580	4,740	22	15.5
1800	.02	5,520	5,590	39	32.5
1800	.2	6,450	6,780	45	30.5
2000	.002	2,800	3,500	14	11.6
2000	.02	3,400	3,760	40	19.5
2000	.2	4,230	4,300	53	63
2100	.002	2.060	3,000	11	14.5
2100	.02	2,830	3,280	38	22
2100	.2	3,370	3,670	59	37.5
		recrystallized (as-extruded + rolled 47% + 1/2300°F)			
1800	.002	20,500	21,200	33.6	6.5
1800	.02	21,200	22,100	20.8	6.9
1800	.2	21,700	23,100	44.6	8.5
2000	.002	18,500	18,800	13	*
2000	.02	18,700	19,800	20.2	7.1
2000	.2	19,700	20,400	30.7	7.3
2100	.002	16,750	17,450	8	4.0
2100	.02	17,400	17,930	13	6.5
2100	.2	18,000	18,940	36	7.5
		commercial bar + 1/2300°F			
1800	.002	20,800	21,200	3	10
1800	.02	22,700	22,900	7	20
1800	.2	24,300	24,800	18	6.4

TABLE 10(continued)

2000	.002	16,300	16,700	1	2.9
2000	.02	17,300	18,100	3	2.6
2000	.2	20,100	20,700	13	5.6
2100	.002	13,900	14,700	1.5	1.5
2100	.02	14,600	16,080	1.5	3.7
2100	.2	17,050	17,600	5	4.0

* broke getting out of grip
gage section .113" x 1.25"

TABLE 11

ACTIVATION ENERGIES AT 2000°F DETERMINED BY TENSILE TESTING

Material	Test Method	ΔH K-cal/mol
as-extruded + 1/2300°F	Conventional	193
	Differential	175
recrystallized (as-extruded + rolled 47% + 1/2300°F)	Conventional	330
	Differential	190
commercial bar + 1/2300°F	Conventional	220
	Differential	160

TABLE 12

ROOM TEMPERATURE TENSILE PROPERTIES

Material	Prop. Limit(psi)	Yield Strength 0.2%Offset(psi)	Ultimate Tensile Strength(psi)	Red.in Area %	Elong.%	Hardness (VHN)
as-extruded	48,850	88,700	103,600	82	11.2	253
commercial bar	41,250	85,750	104,750	62	12	240
recrystallized (as-extruded + rolled 47% longitudinally + 1/2300°F)	28,150	43,875	74,750	75	15.1	188

TABLE 13

RECRYSTALLIZATION IN AS-EXTRUDED TD NICKEL

AFTER ONE HOUR HEAT TREATMENTS

Rolling Reduction (%)	% Recrystallized 2400°F	2300°F	2000°F
	Longitudinal Pass		
21	91	95	0
37	97	99	30
59	99	99	11
74	97(0)(80)	100(0)(80)	16
85	100(0)(50)	100(0)(50)	50(0)(10)
90	0	0	0
	Transverse Pass		
20	100	85	0
36	98	65	1
59	95	90	5
74	95	95	25
85	100(50)(80)* **	80(0)(60)	2
88	100(0)(80)	100(0)(60)	0
	Radial Pass		
21	95	5	0
34	95	30	0
57	90	85	3
70	60	30	1
91	10	5	2

Swaging Reduction (%)	2400°F
14	0
26	0
45	0
59	0
75	0
82	0
90	0
95	0

* = % recrystallized at surface
** = % recrystallized overall

TABLE 14

RECRYSTALLIZATION IN COMMERCIAL TD NICKEL

BAR AFTER ONE HOUR HEAT TREATMENTS

Rolling Reduction (%)	% Recrystallized 2400°	2300°	2000°	1500°	1250°	1000°F
			Longitudinal Pass			
21	0					
37	0					
59	0					
74	0					
82	0					
87	0					
			Transverse Pass			
22		0	0	0	0	0
37		99	97	25	2	0
59		100	100	80	52	5
74		100	100	95	95	0
83		100	100	100	100	0
87		100	100	100	100	0
			Radial Pass			
22	0	0	0			
38	0	0	0			
60	2	0	0			
73	35 (45)*	(40)**	20 (55)	(40)	0	
85	100		30 (50)	(40)	5	
			Swaging Reduction (%)			
	2400°F					
14	0					
26	0					
45	0					
59	0					
75	0					
82	0					
90	0					
95	0					

* = % recrystallized at surface
** = % recrystallized overall

TABLE 15

X-RAY INTENSITY AND HALF PEAK WIDTH OF CENTRAL FIBER TEXTURE IN TD NICKEL

Material	Intensity of (111) Line	Half Width of (111) Line (° of Tilt)	Intensity of (200) Line	Half Width of (200) Line (° of Tilt)	Ratio of (111)/(200) Components*
as-extruded	.7	22.5	.75	19	.65
" " + swaged 28%	3.2	13	3.4	11	.62
" " + swaged 60%	12.5	8.8	10.5	8.8	.79
" " + swaged 84%	32.5	6.1	18.8	6.1	.98
commercial bar	38.5	6.1	29.5	5.9	.76
" " + swaged 28%	37.5	5.9	22	6.1	.92
" " + swaged 60%	44	5.9	22.5	5.9	.97
" " + swaged 84%	45	5.9	25	6.1	.97

* $\dfrac{\text{Max I(111) X Half Width (111) X Multiplicity Factors X Lorentz Polarization Factors}}{\text{Max I(200) X Half Width (200)}}$

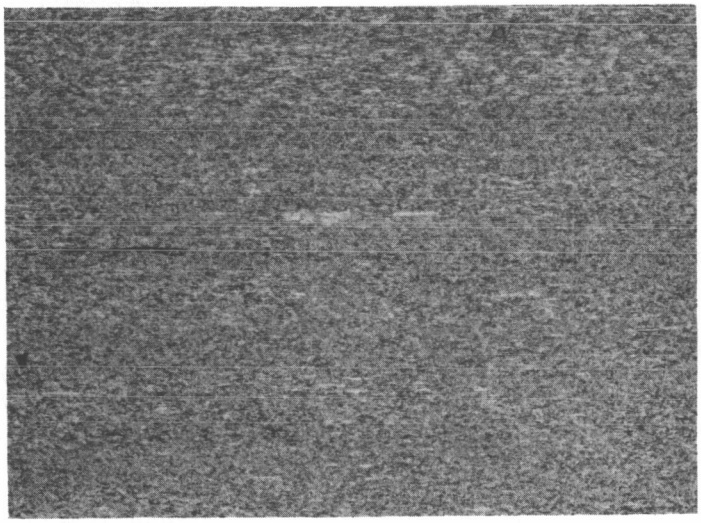

500X

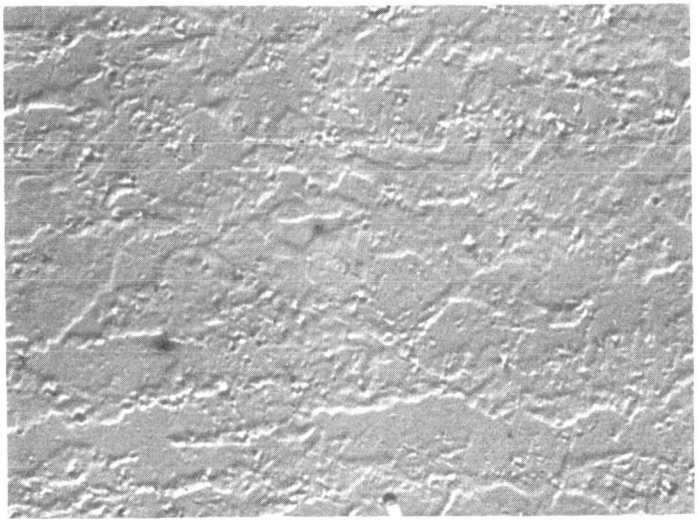

10,000X

Figure 1. Optical and Electron Microstructure of As-Extruded TD Nickel

500X

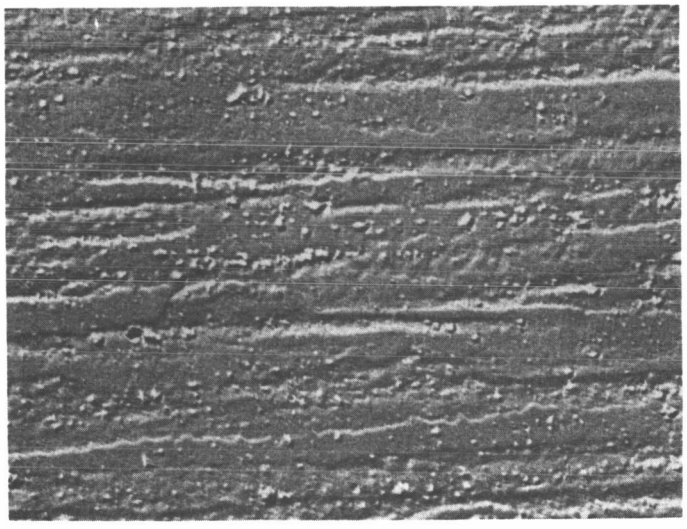

10,000X

Figure 2. Optical and Electron Microstructure of Commercial One Inch TD Nickel Bar.

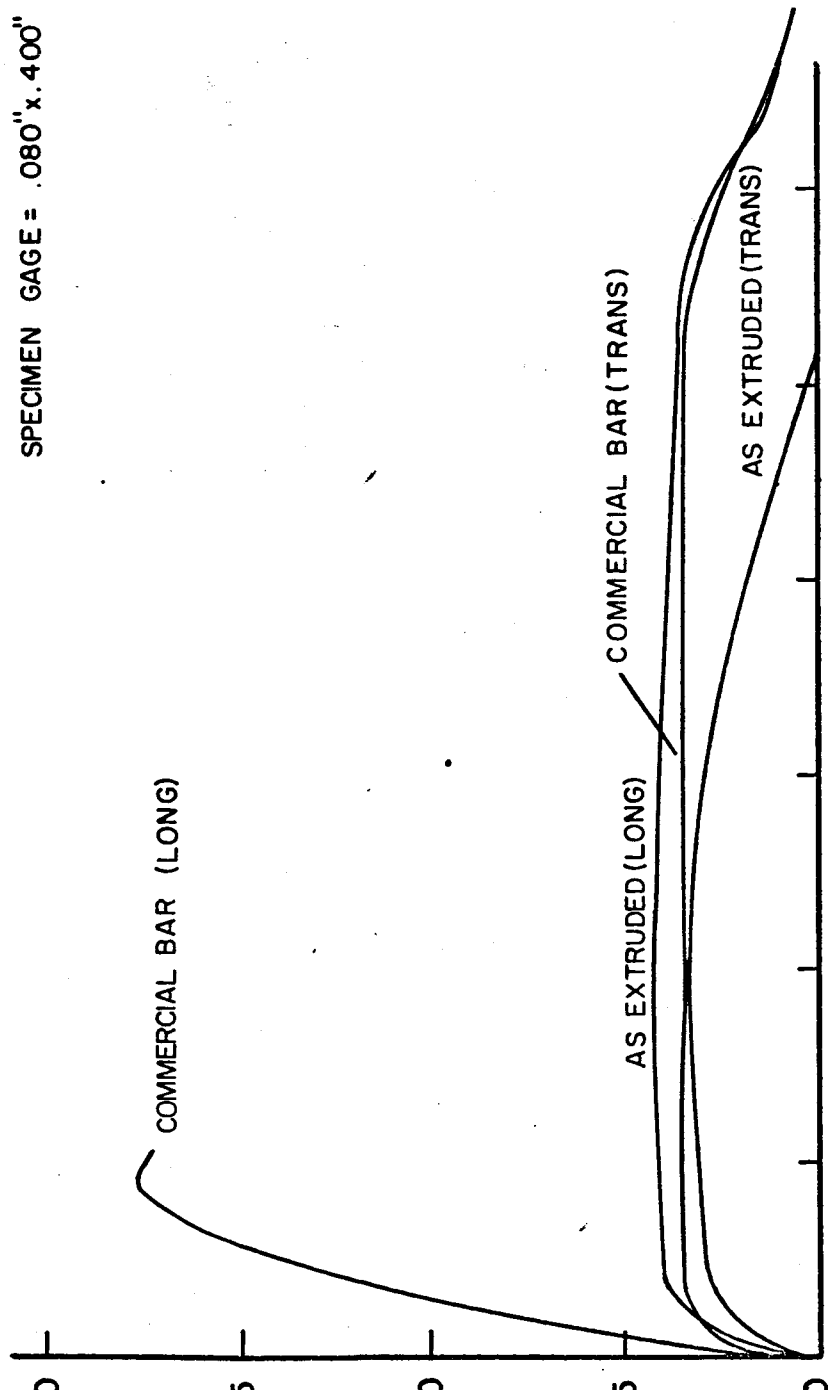

FIGURE 3: LOAD VERSES ELONGATION FOR 2000°F TENSILE TESTS.

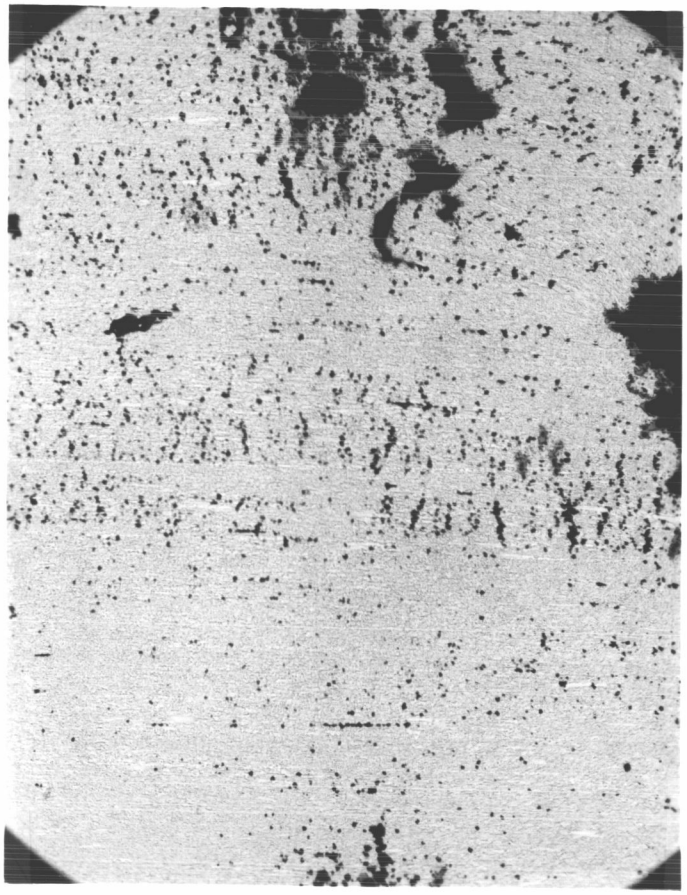

100X
Unetched

Figure 4. Internal Cracking of As-Extruded TD Nickel After 2000°F Tensile Test.

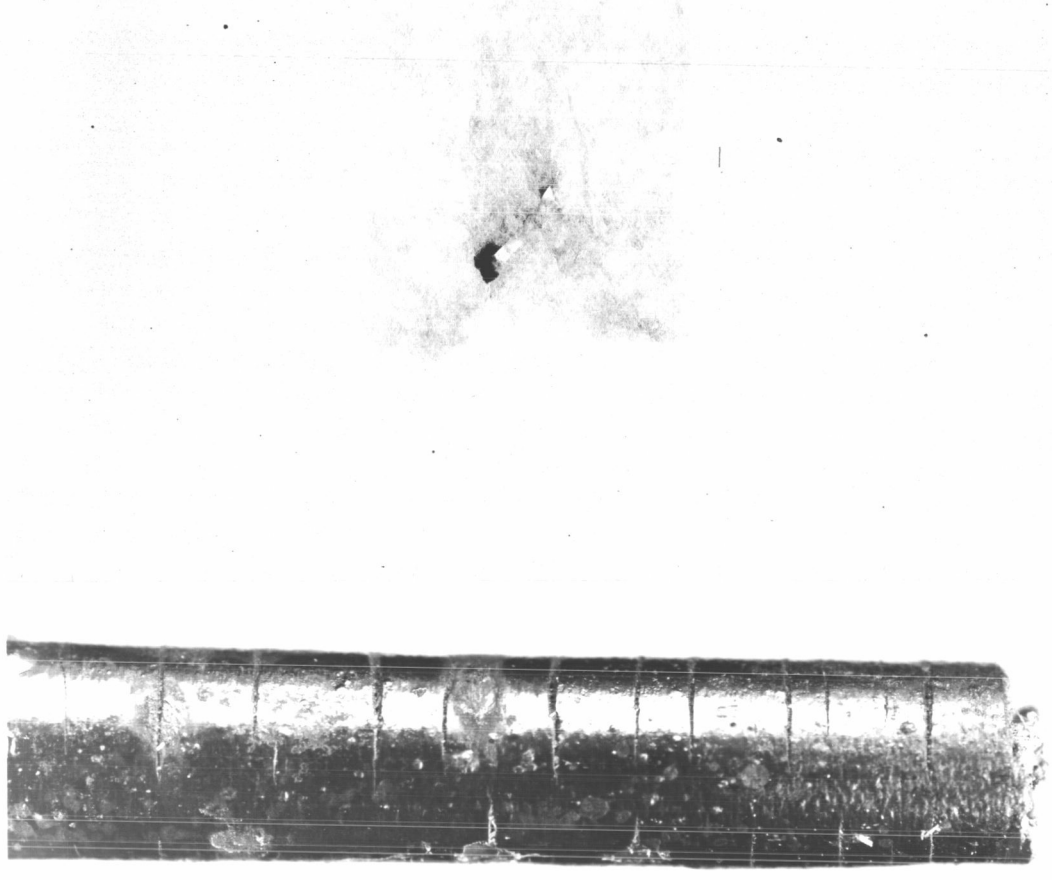

Figure 5. Fracture Surface of Commercial TD Nickel Bar Tested in Transverse Direction at 2000°F. 15X

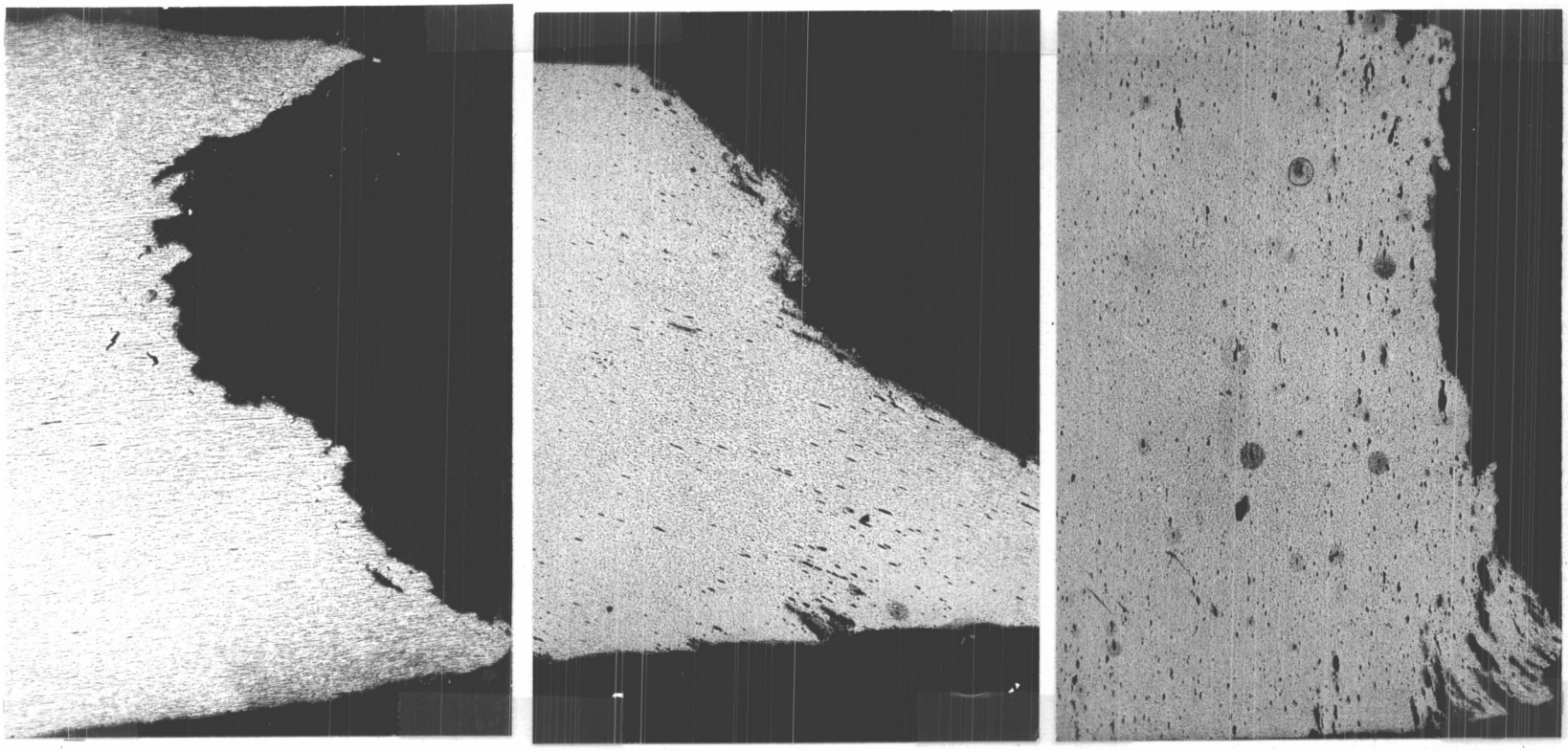

Longitudinal 100X 45° 100X Transverse 100X

Figure 6. Internal Cracking as a Function of Specimen Orientation for Commercial TD Nickel Bar Tensile Tested at 2000°F.

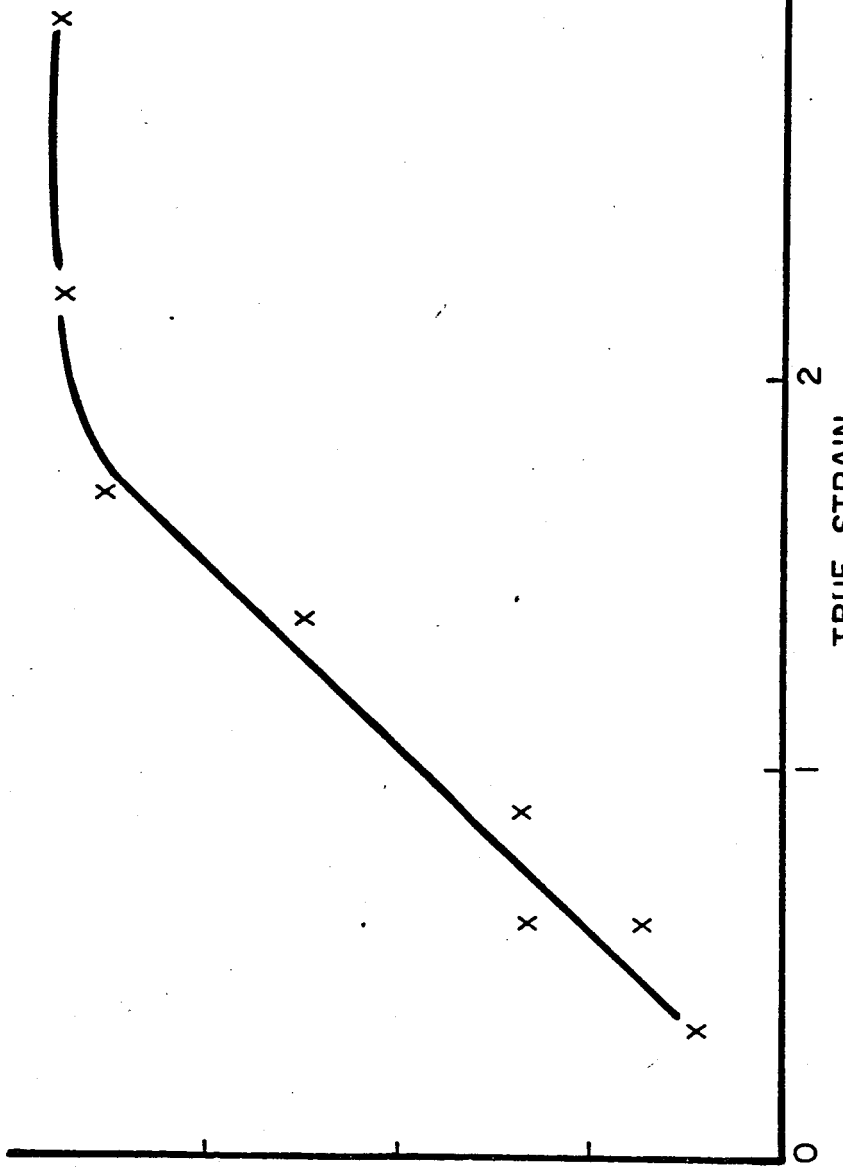

FIGURE 7: EFFECT OF COLD SWAGING ON THE TENSILE STRENGTH OF AS-EXTRUDED TD NICKEL.

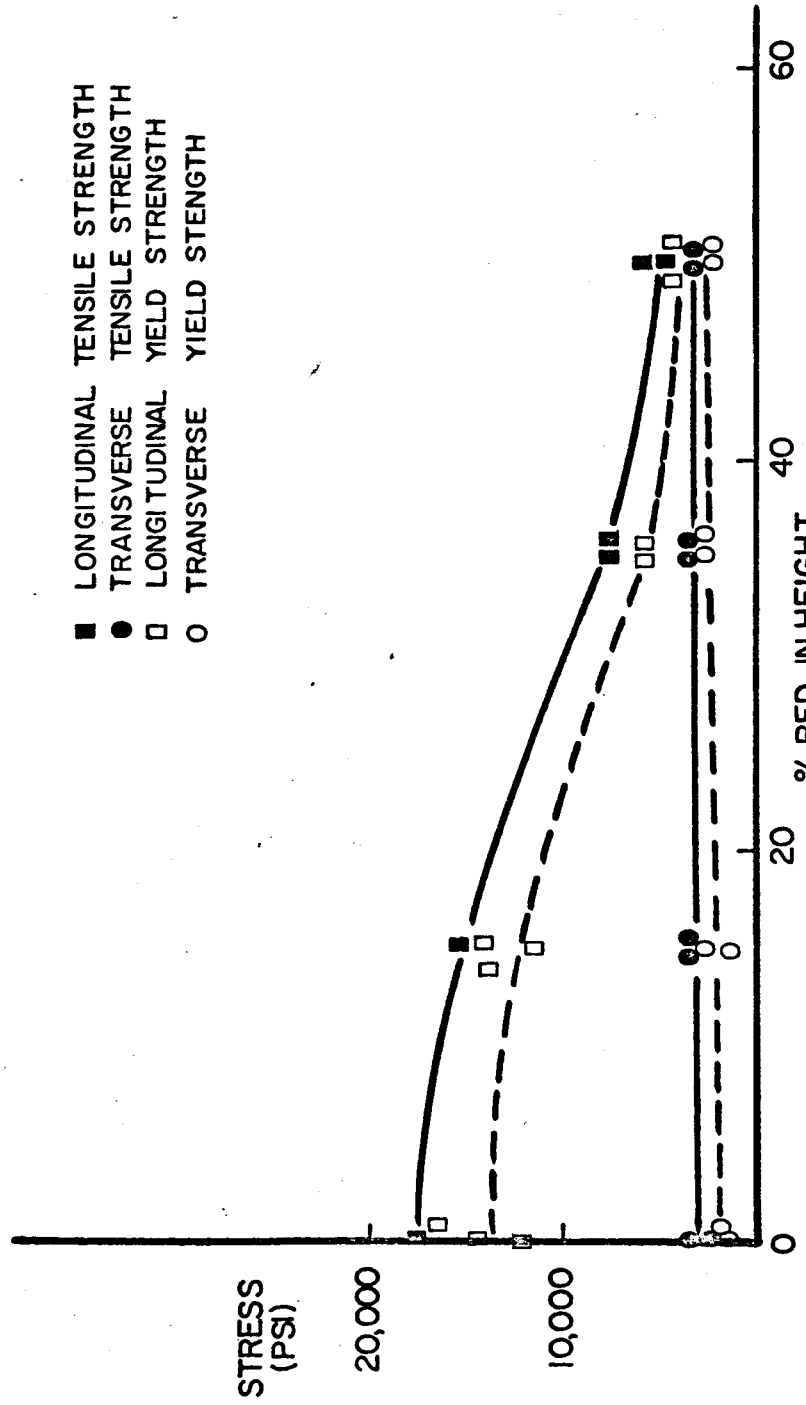

FIGURE 8: EFFECT OF UPSET FORGING ON 2000°F STRENGTH.

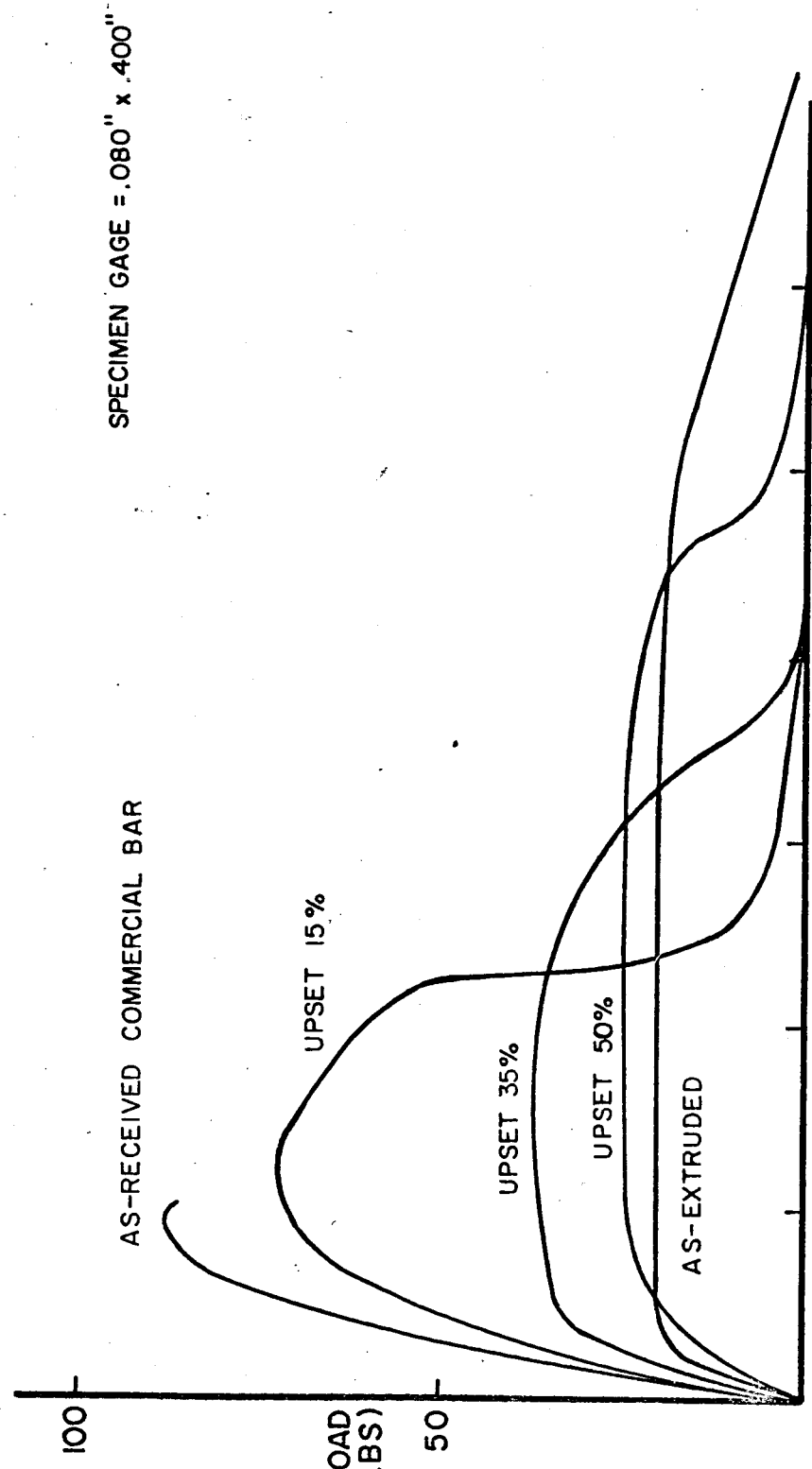

FIGURE 9: EFFECT OF UPSET FORGING ON STRESS-STRAIN BEHAVIOR OF COMMERCIAL TD NICKEL BAR AT 2000°F. LONGITUDINAL TEST DIRECTION.

100X
Longitudinal
Test

Figure 10. Internal Cracking Found After 2000°F Tensile Test of Sample Upset 50% at Room Temperature.

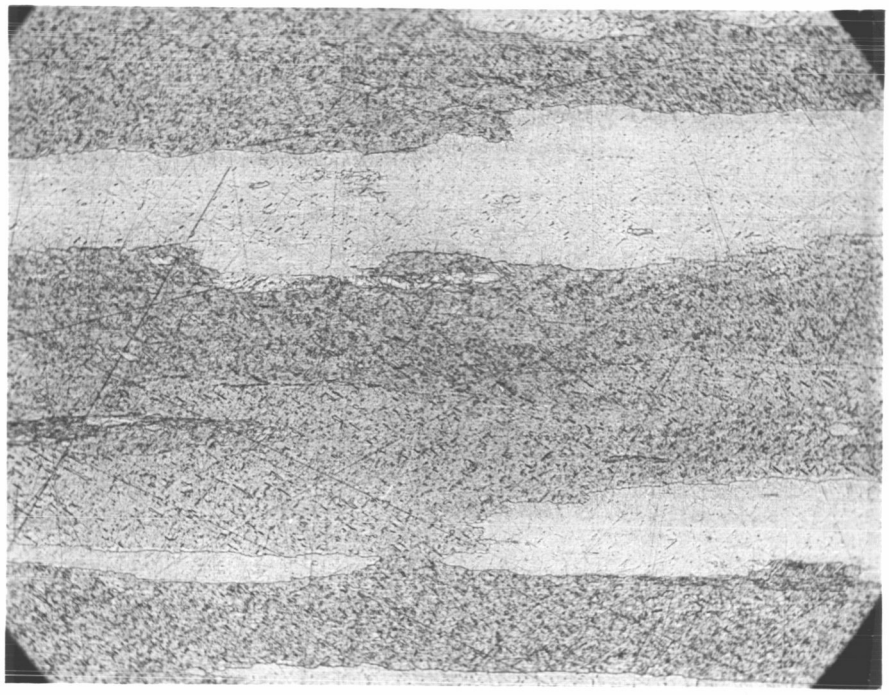

100X

Figure 11. Typical Recrystallized Microstructure (As-Extruded + Longitudinal Rolled 47% + 1/2300°F).

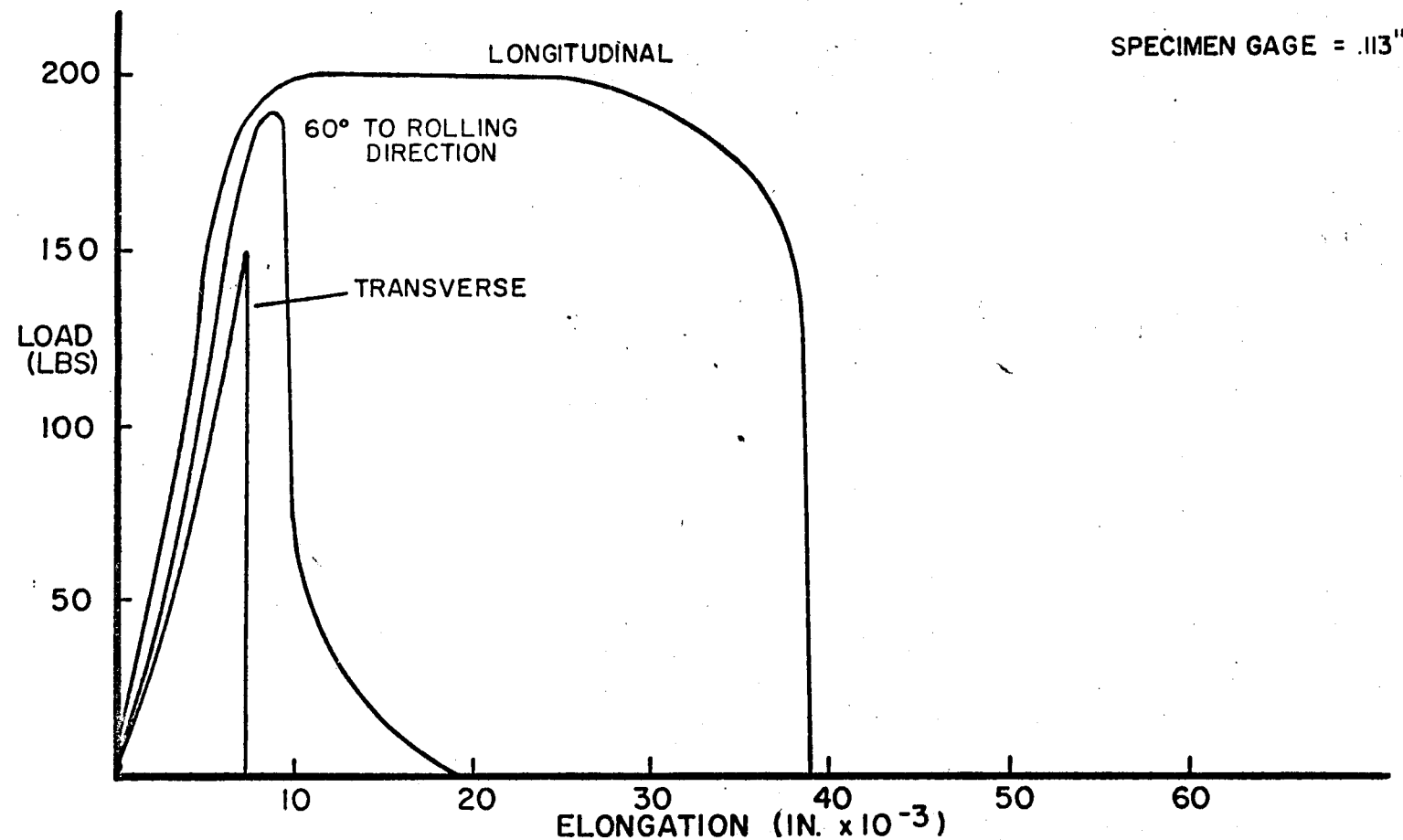

FIGURE 12: EFFECT OF TEST DIRECTION ON STRESS-STRAIN BEHAVIOR OF RECRYSTALLIZED TD NICKEL AT 2000° F

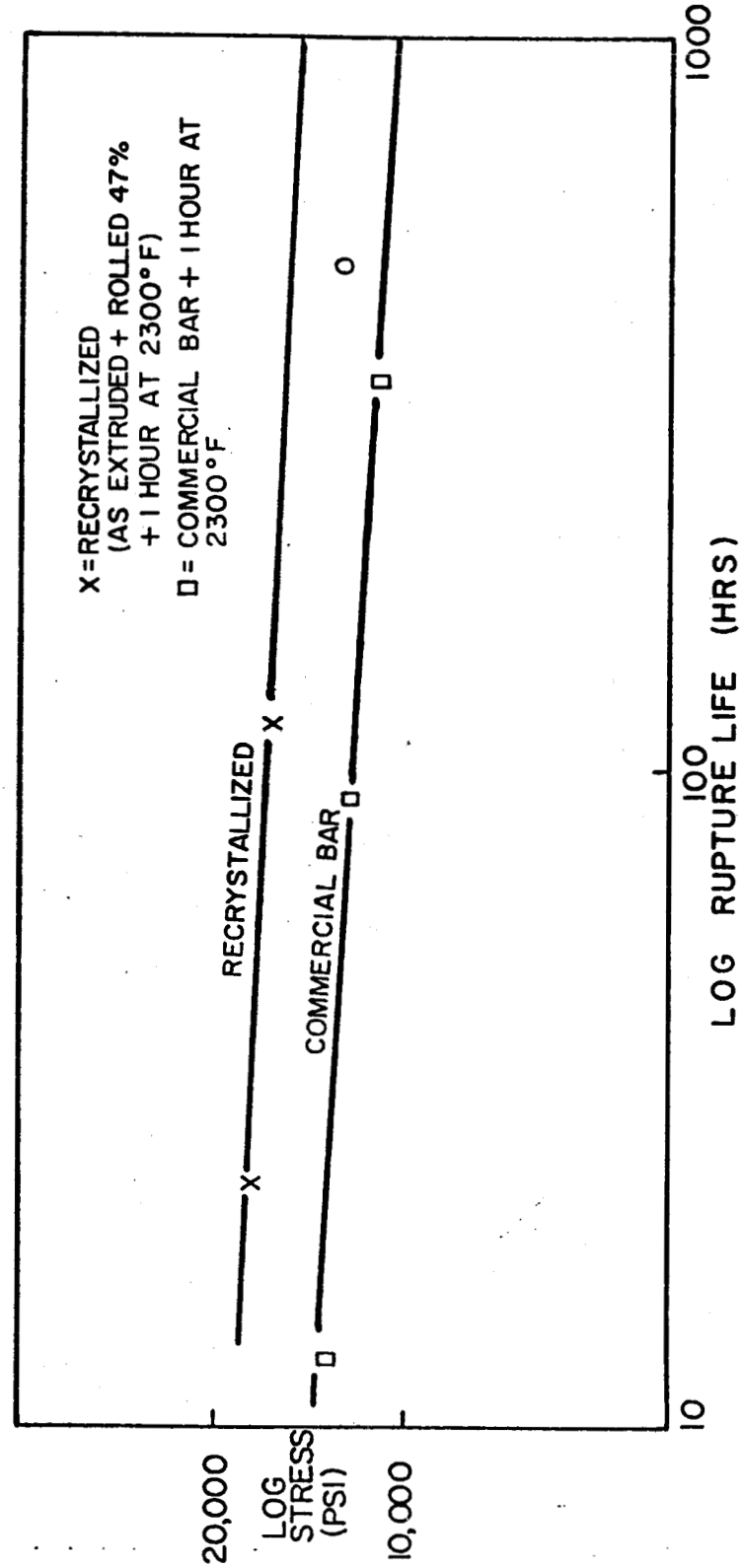

FIGURE 13: LOG STRESS VERSUS LOG RUPTURE LIFE AT 1950°F

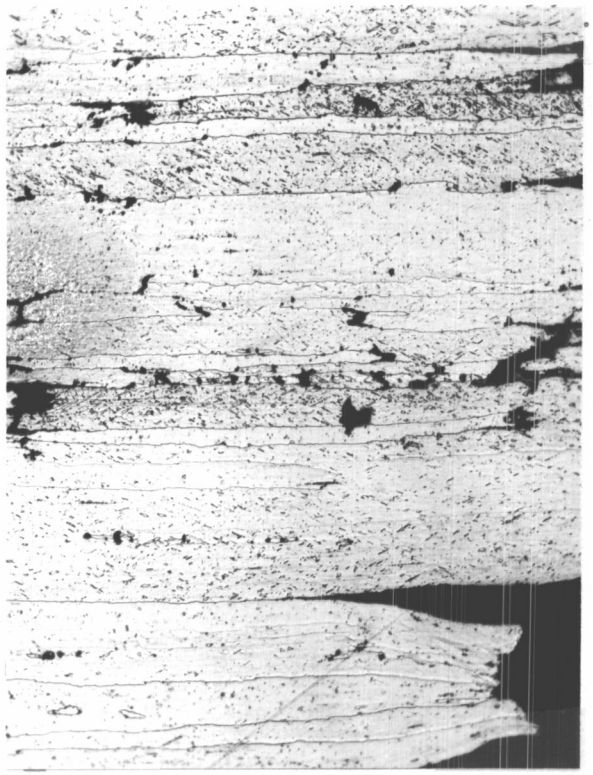

Rolled 50% L 100X

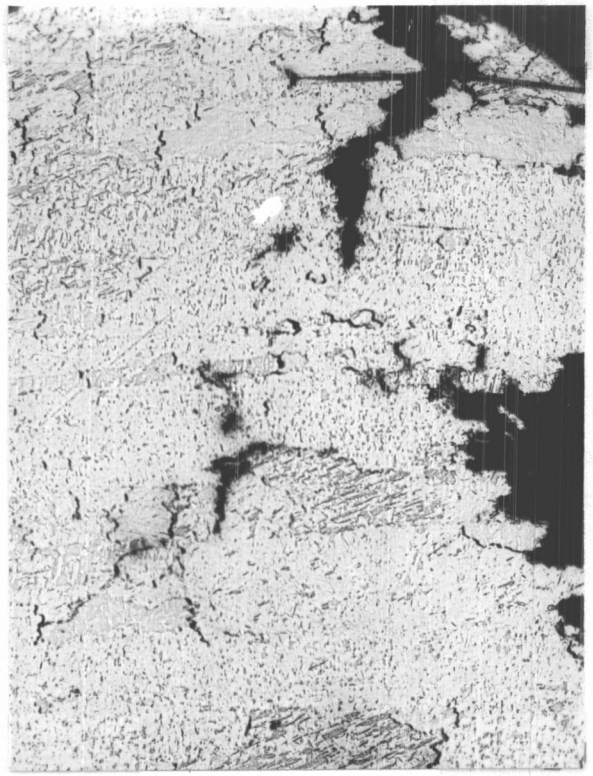

Rolled 50% T 100X

Figure 14. Effect of Prior Rolling Direction on 2000°F Tensile Fracture of Recrystallized TD Nickel.

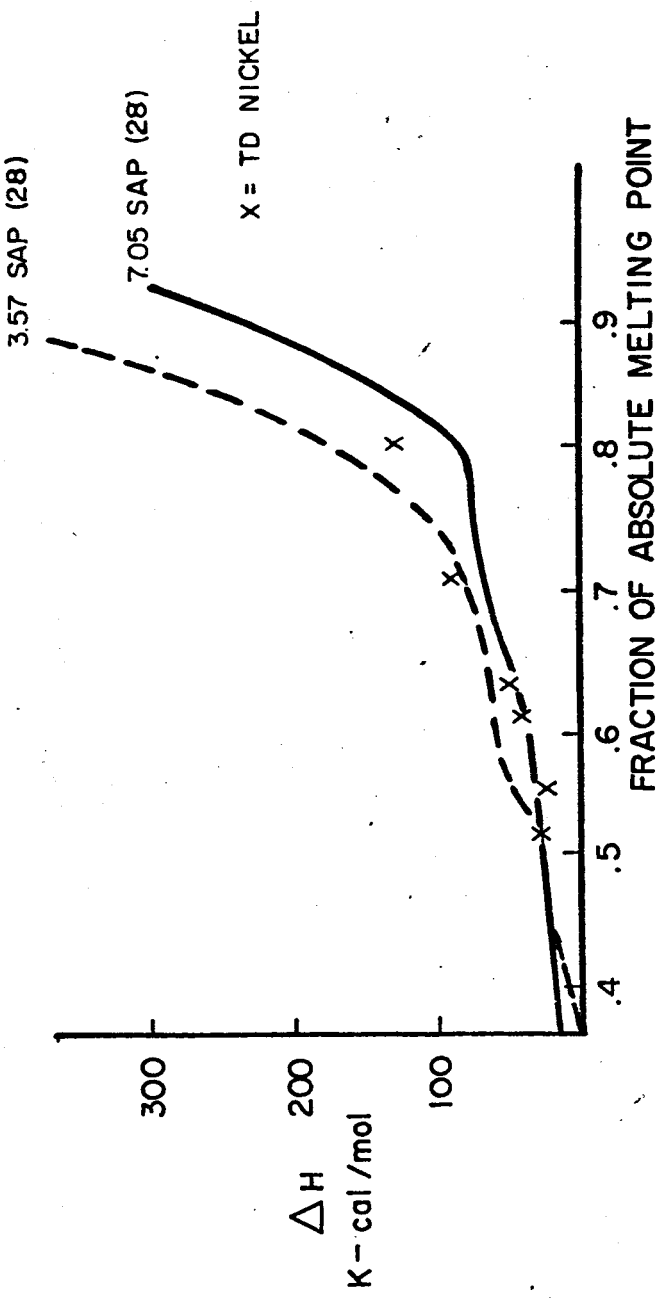

FIGURE 15: ACTIVATION ENERGY AS A FUNCTION OF TEMPERATURE.

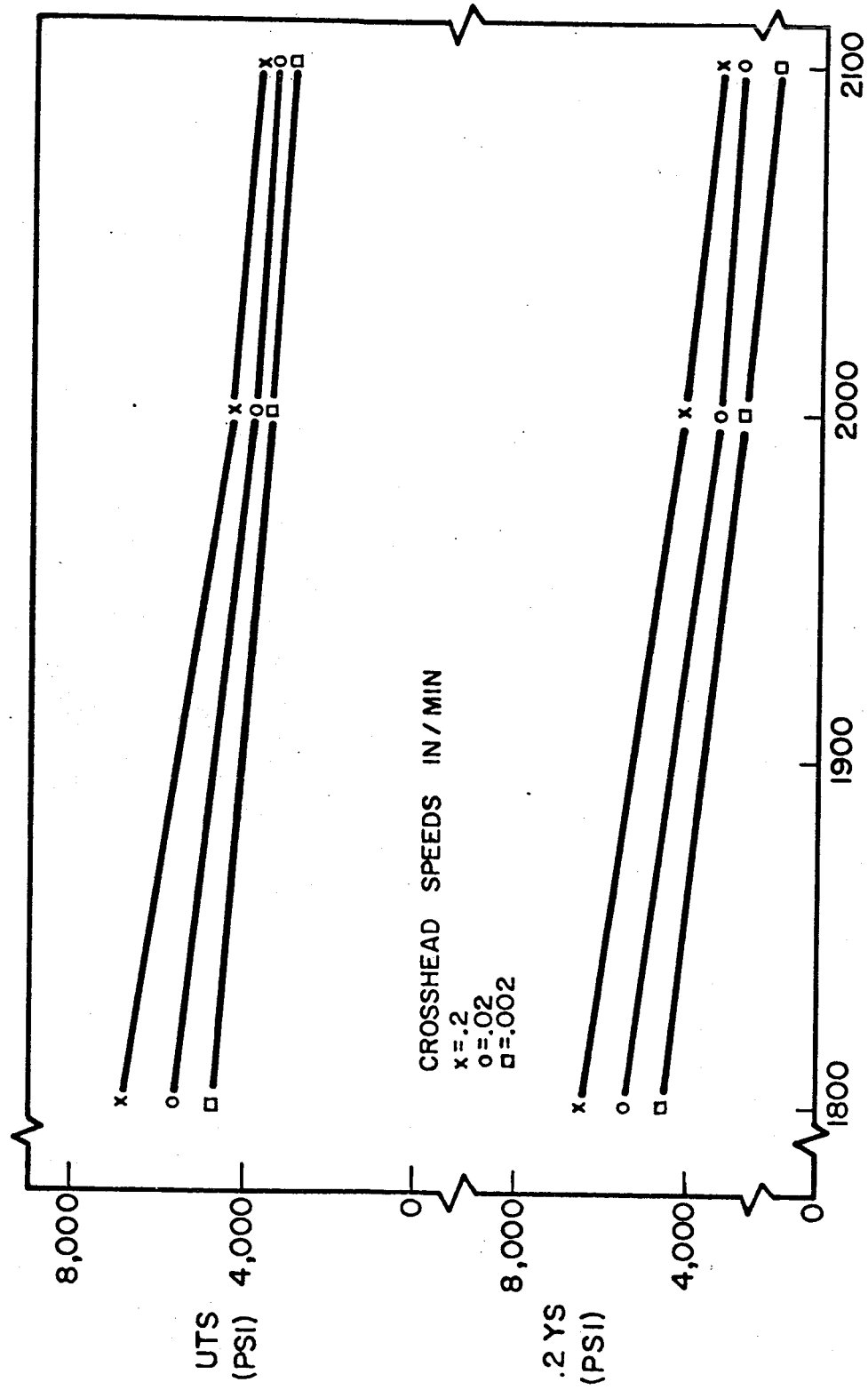

Figure 16. Tensile Properties of As-Extruded TD Nickel Annealed One Hour at 2300°F.

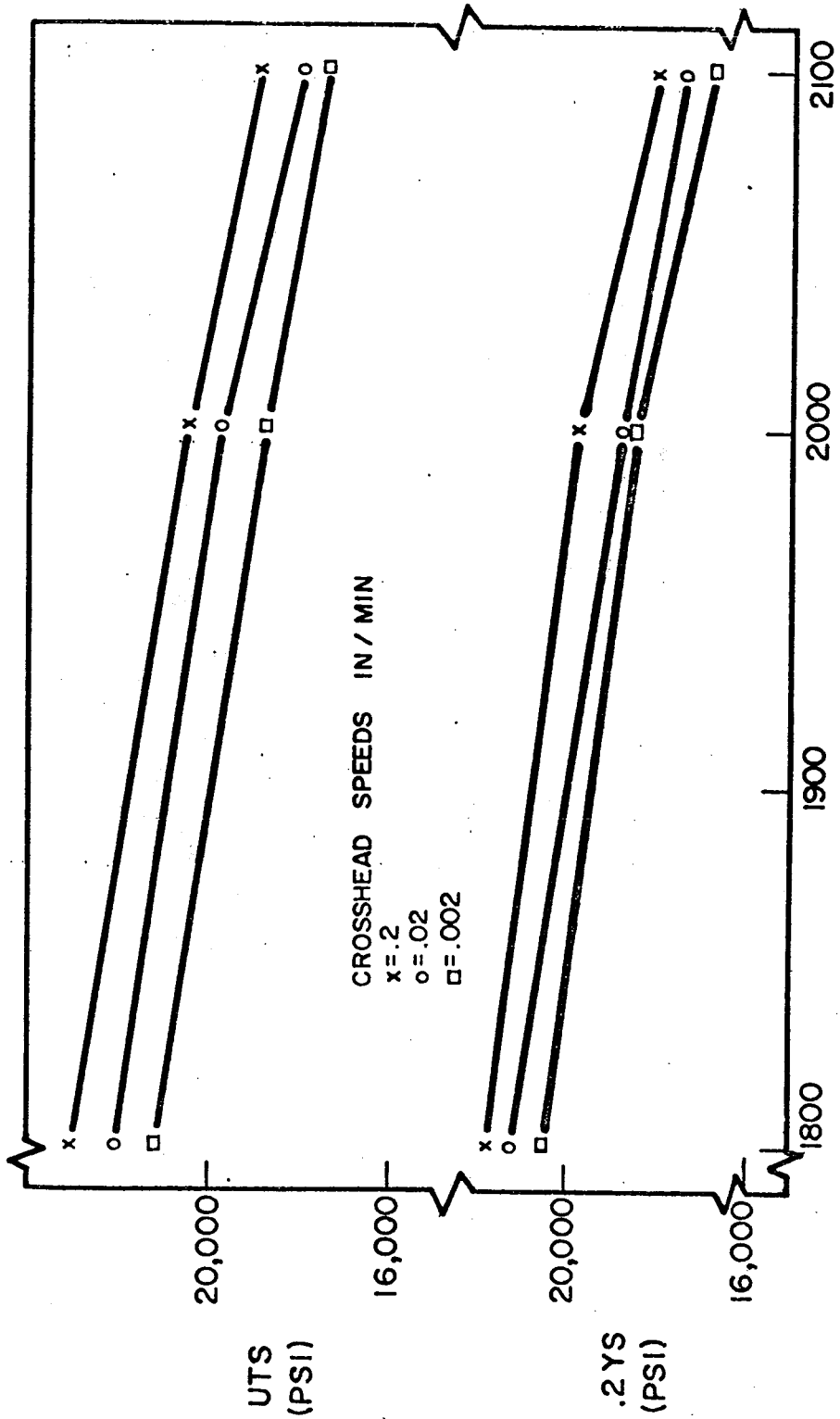

Figure 17. Tensile Properties of Recrystallized TD Nickel (As-Extruded + Rolled 47% in Longitudinal Direction + 1 hour at 2300°F)

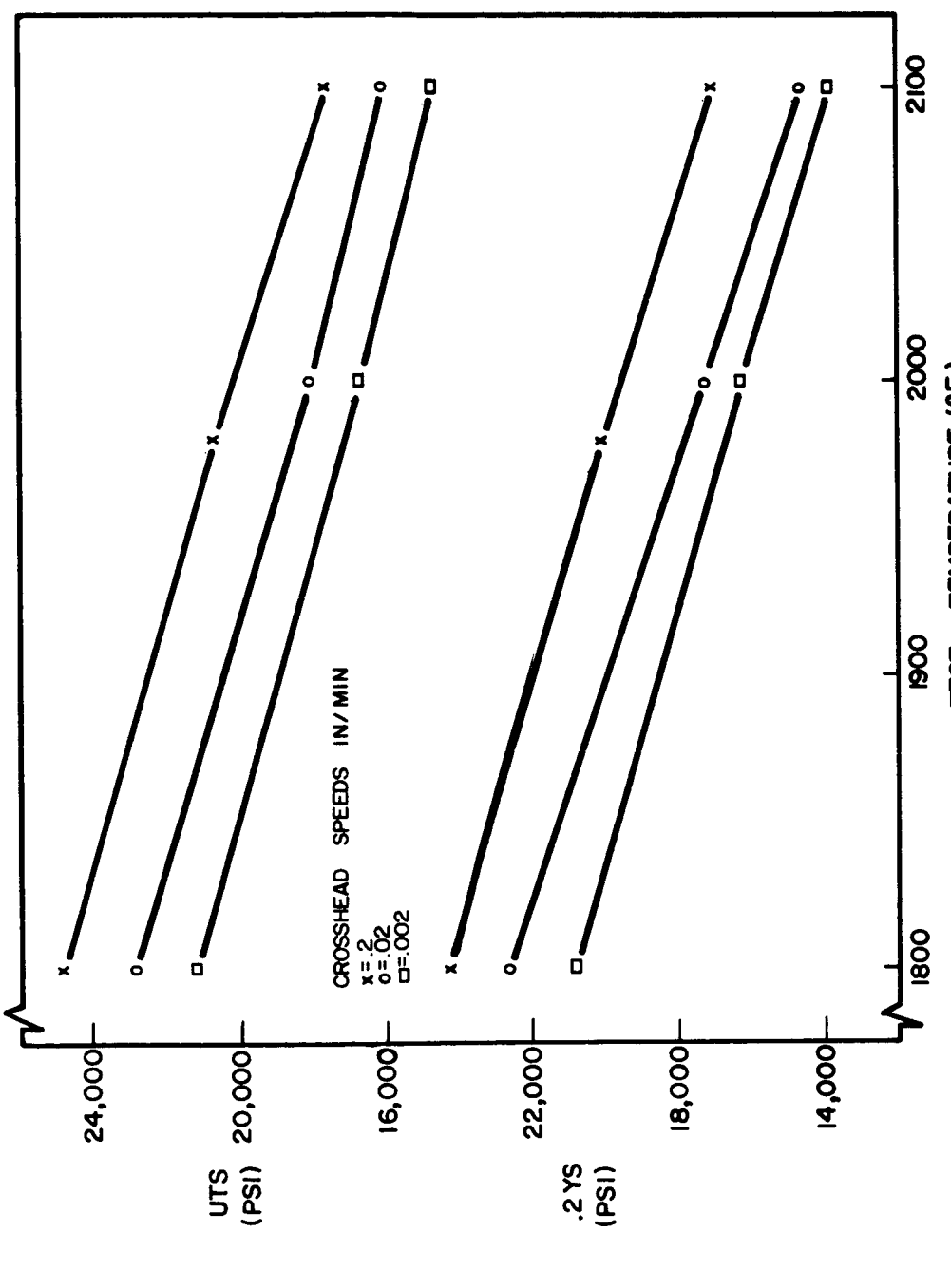

Figure 18. Tensile Properties of Commerical TD Nickel Bar Annealed One Hour at 2300°F.

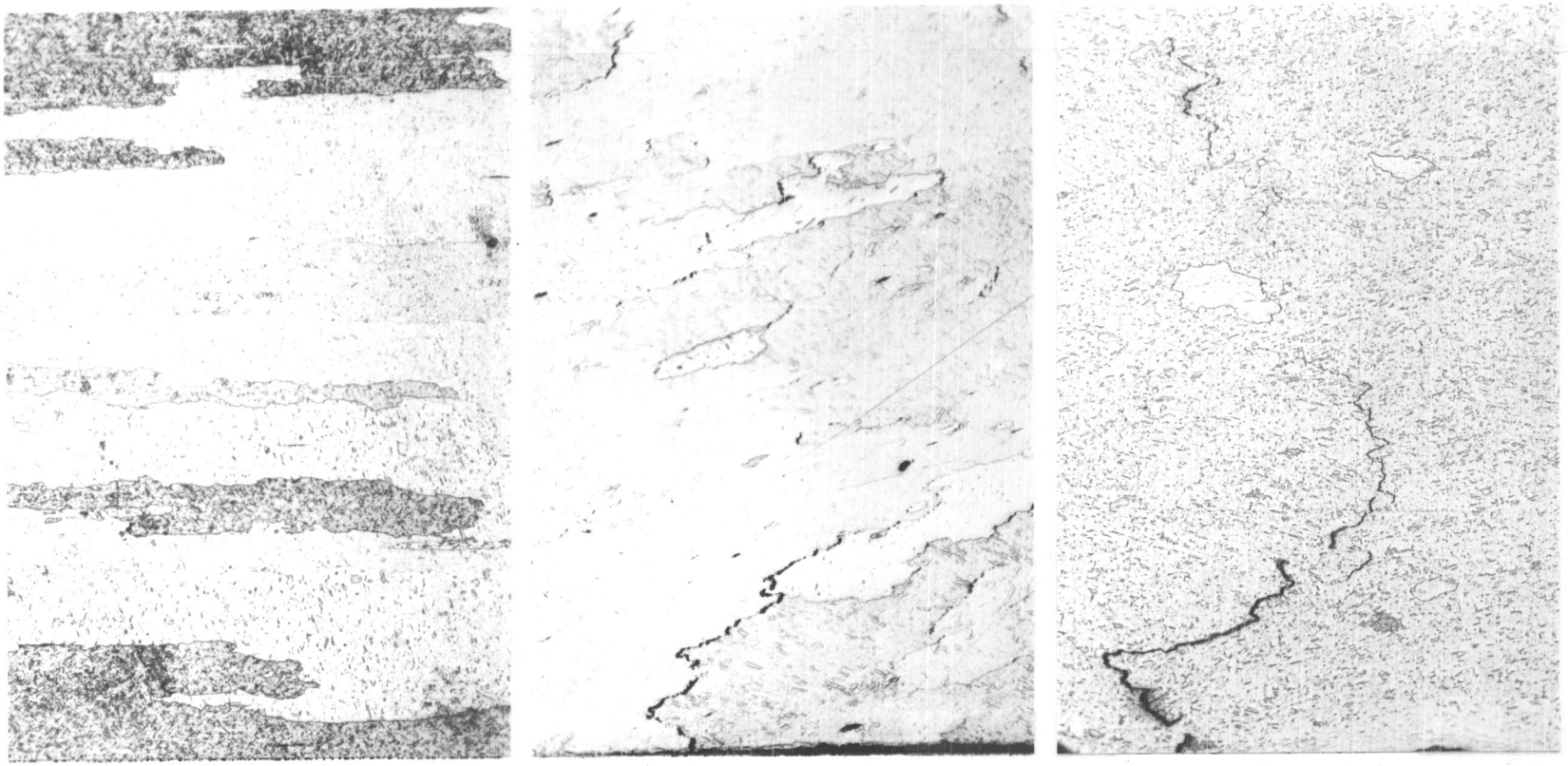

Longitudinal Test 100X

60° to Rolling Direction 100X

Transverse Test (.1% Strain) 100X

Figure 19. Structure of Recrystallized Specimens Strained to 0.2% Offset Yield Stress at 2000°F.

250X
Unetched

Figure 20. Grain Boundary Sliding on Surface of Recrystallized Specimen Tested to 0.2% Offset Yield Stress at 60° to Rolling Direction.

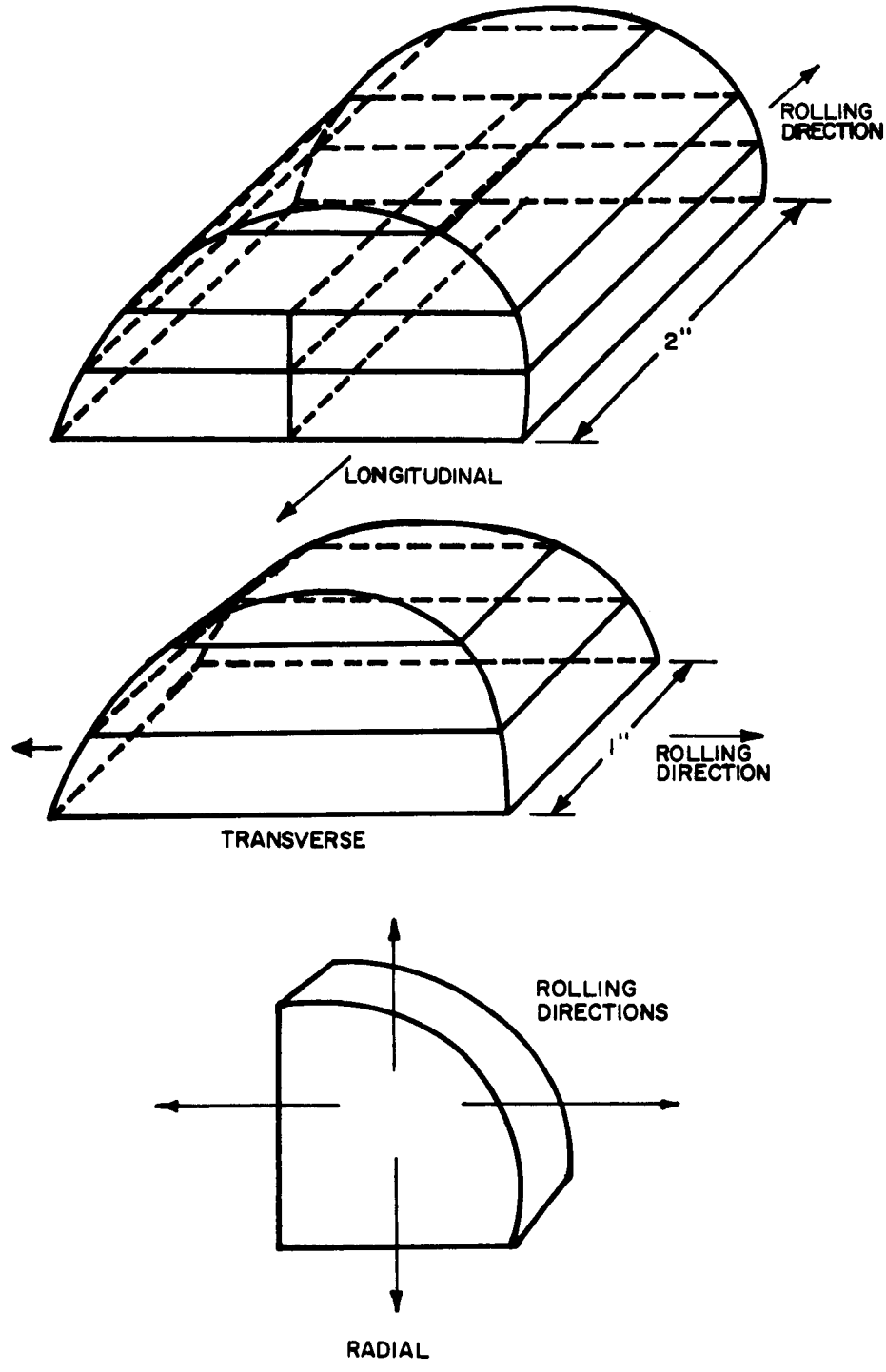

Figure 21. Pieces Sectioned for Rolling from As-Extruded TD Nickel

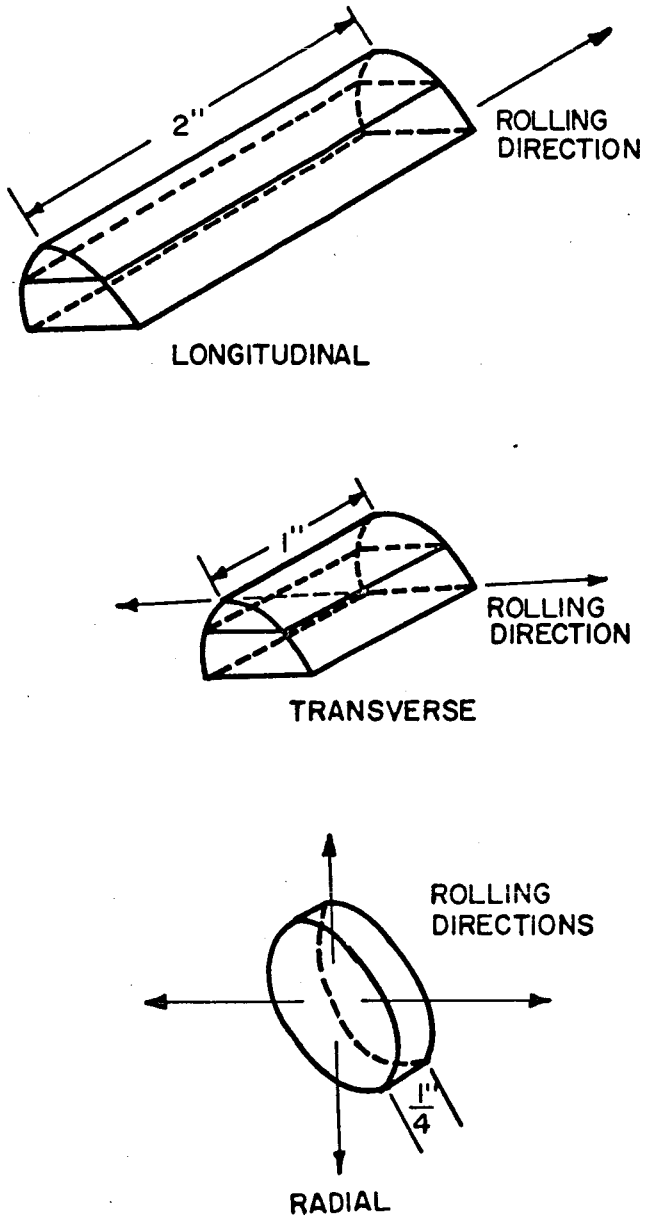

Figure 22. Pieces Sectioned For Rolling From Commercial One Inch TD Nickel Bar

37% Reduction

85% Reduction

90% Reduction

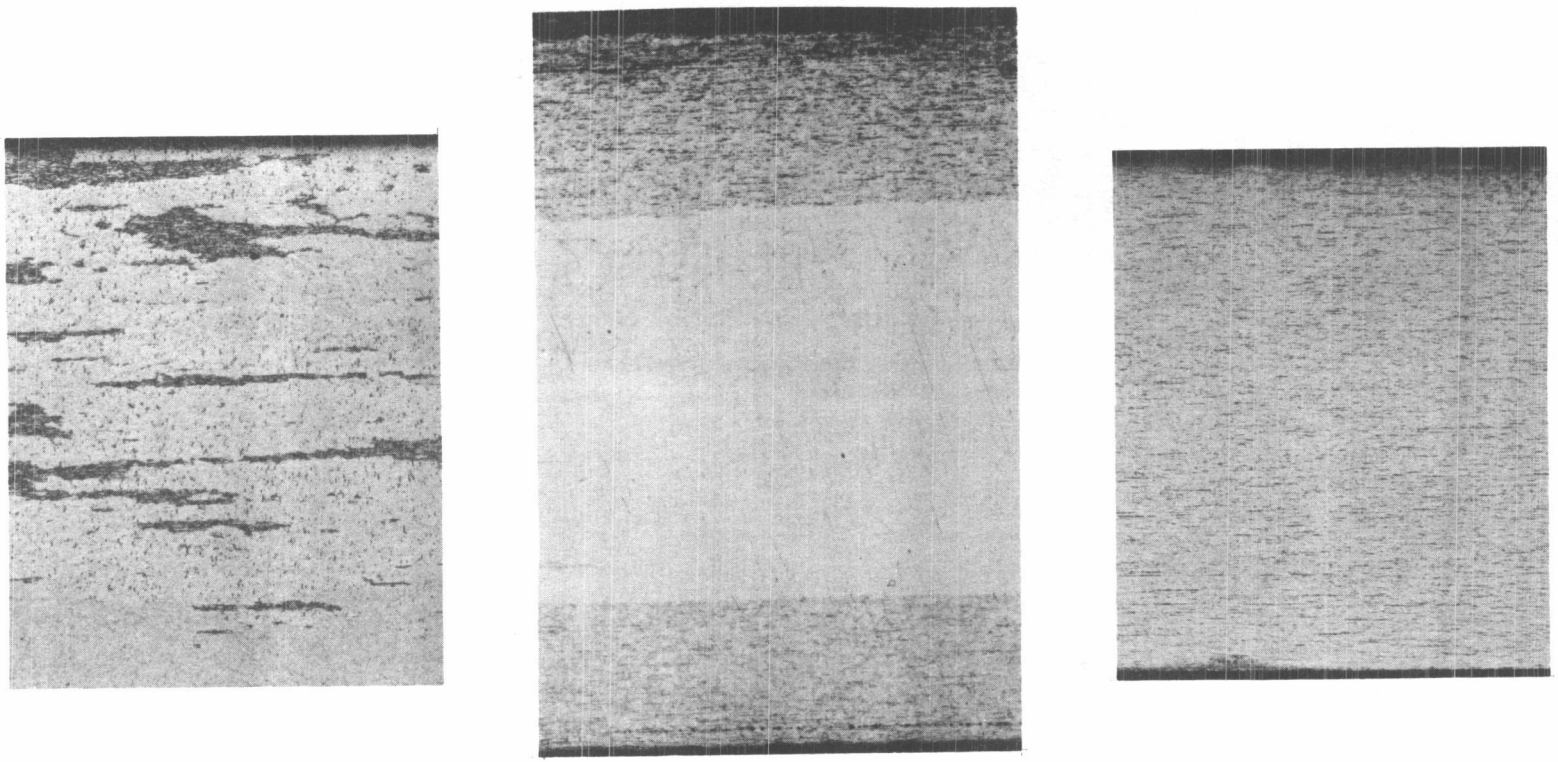

100X

100X

100X

Figure 23. Development of Unrecrystallized Surface Layer During Longitudinal Rolling Passes of As-Extruded Material.

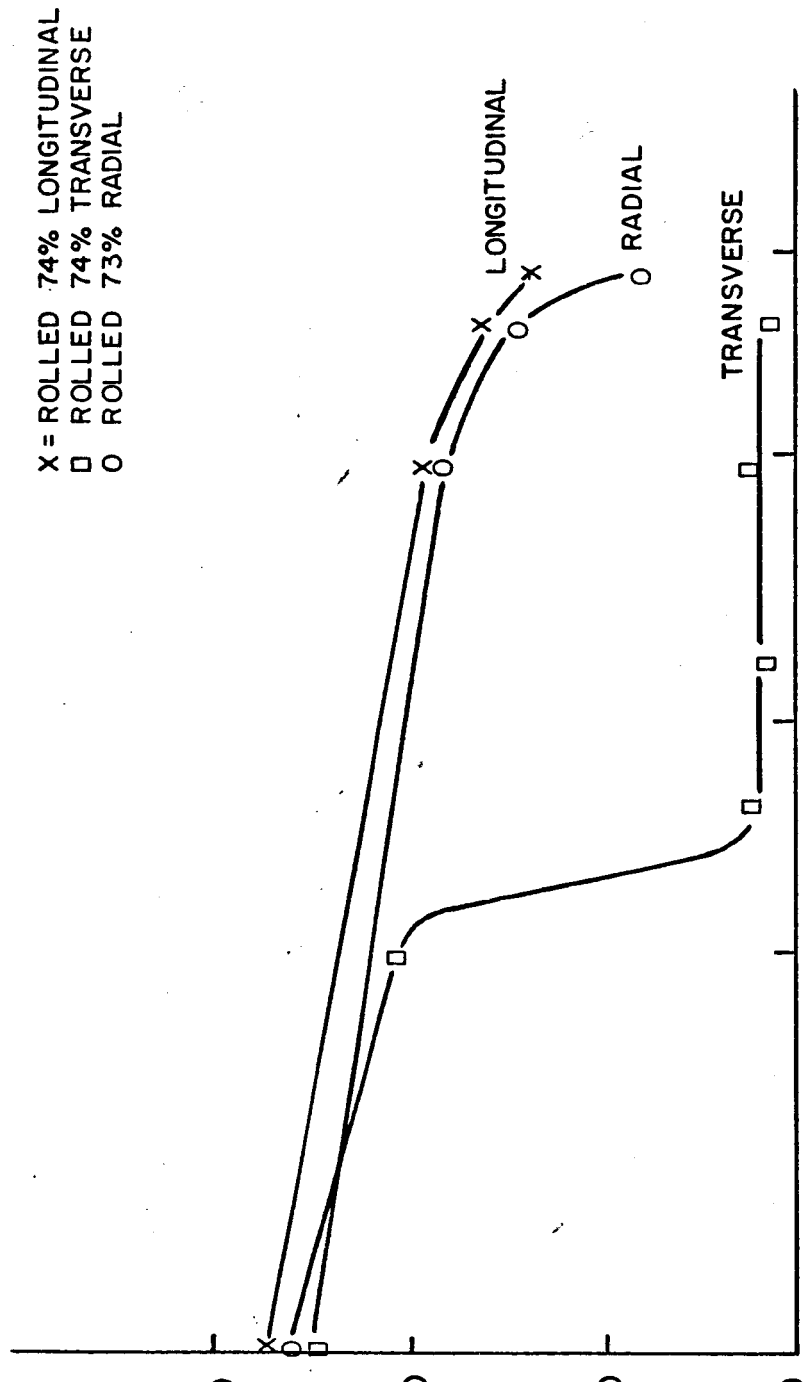

FIGURE 24: EFFECT OF ROLLING DIRECTION ON RECRYSTALLIZATION OF COMMERCIAL TD NICKEL BAR.

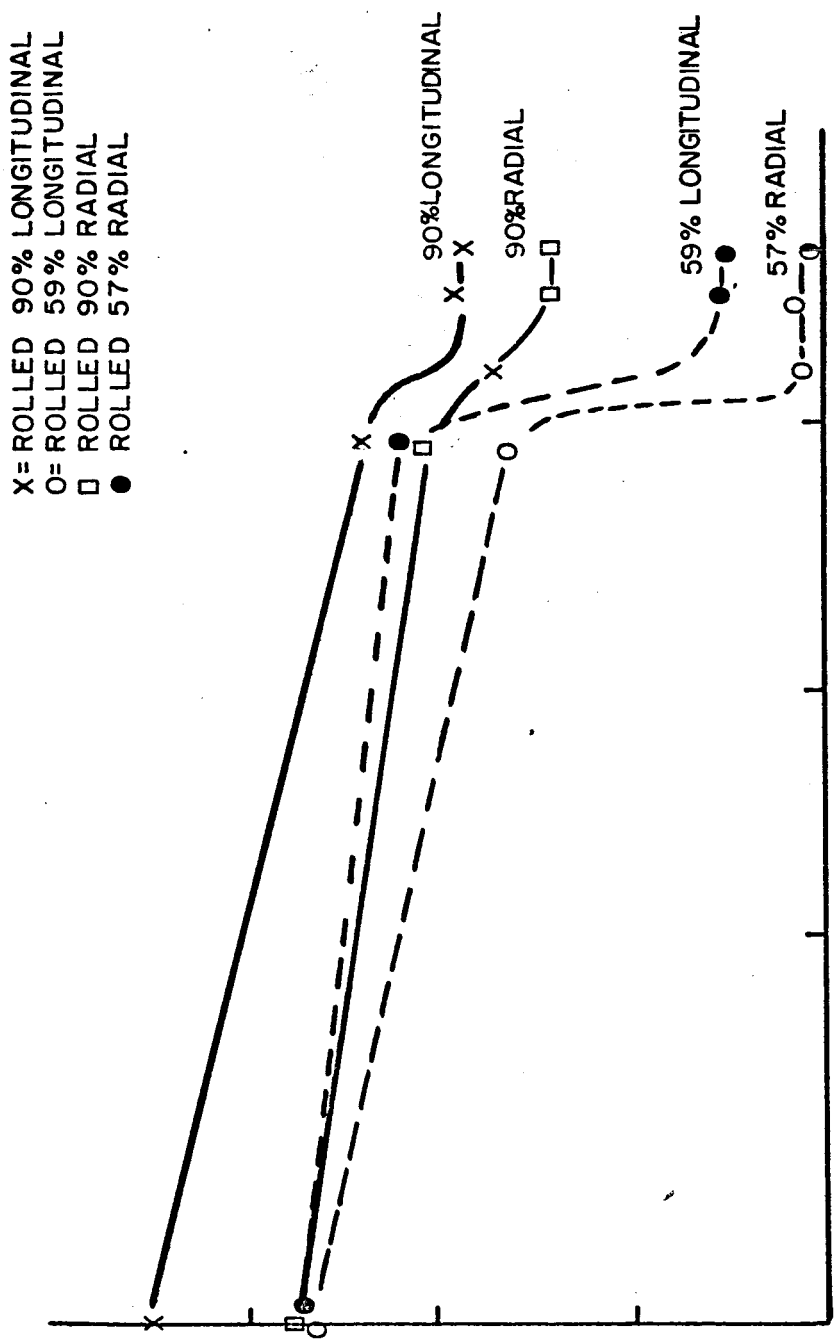

FIGURE 25: EFFECT OF ROLLING REDUCTION ON RECRYSTALLIZATION OF AS-EXTRUDED TD NICKEL.

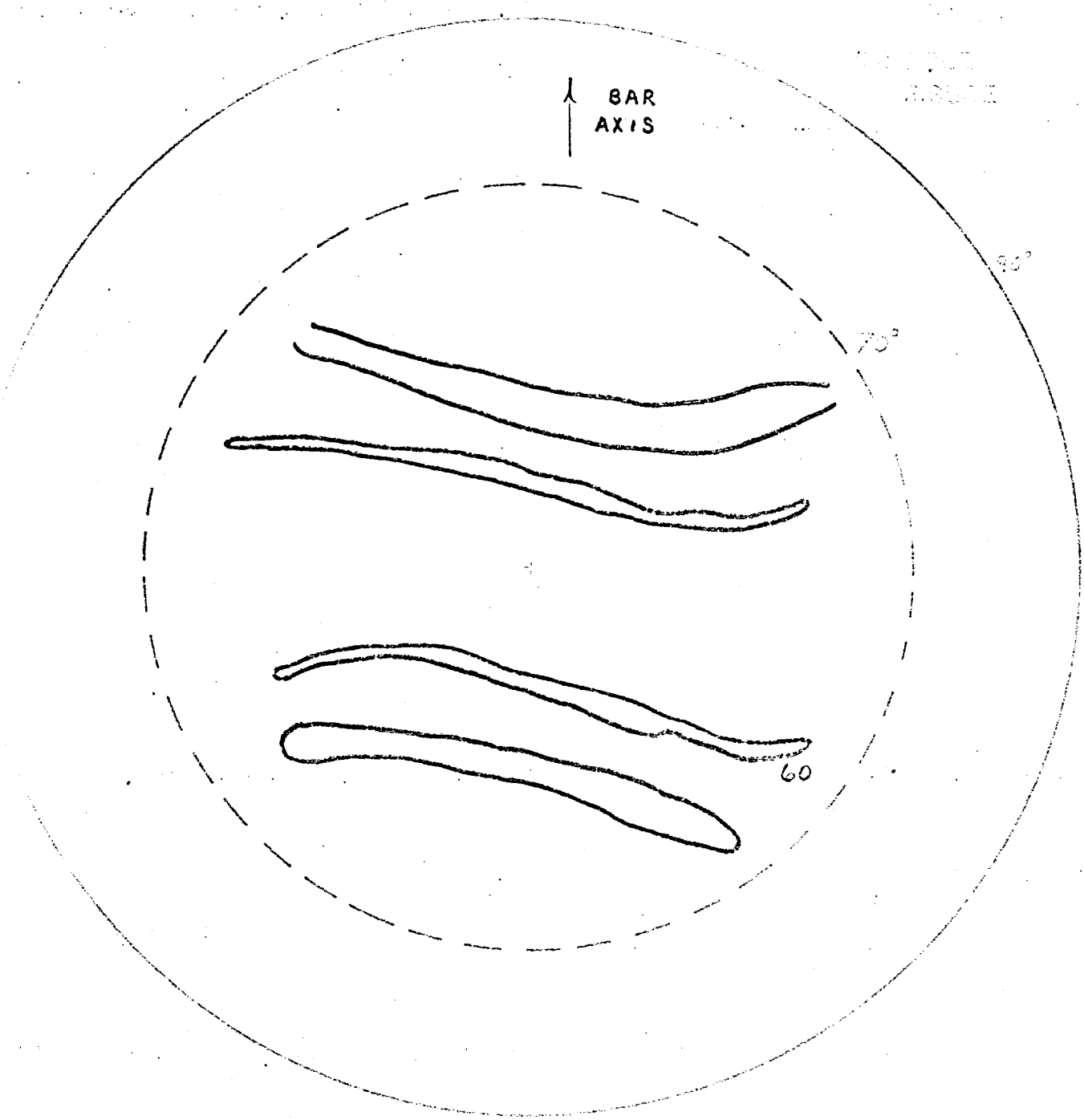

Figure 26. Pole Figure of Commercial TD Nickel Bar.

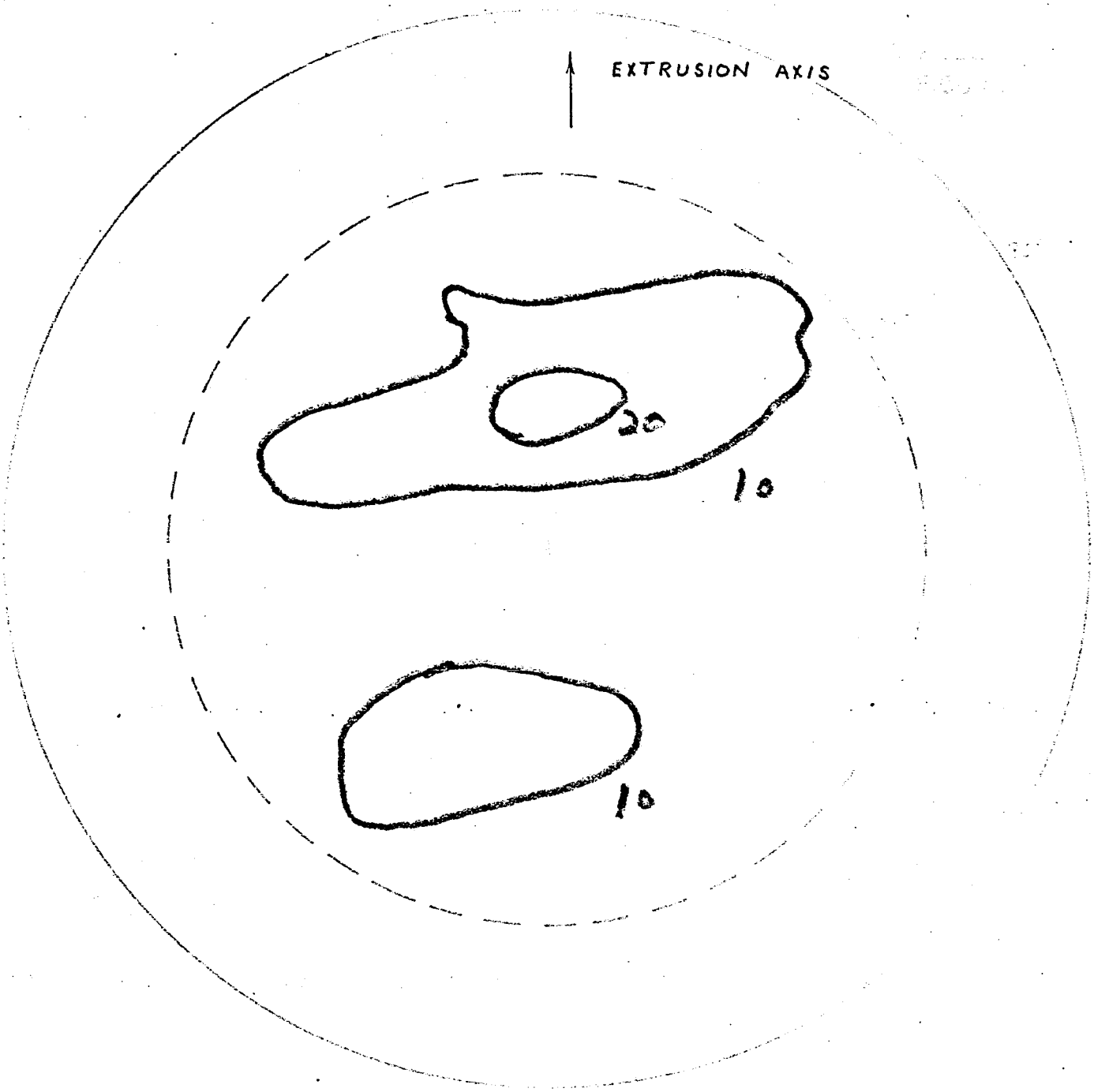

Figure 27. Pole Figure of As-Extruded TD Nickel.

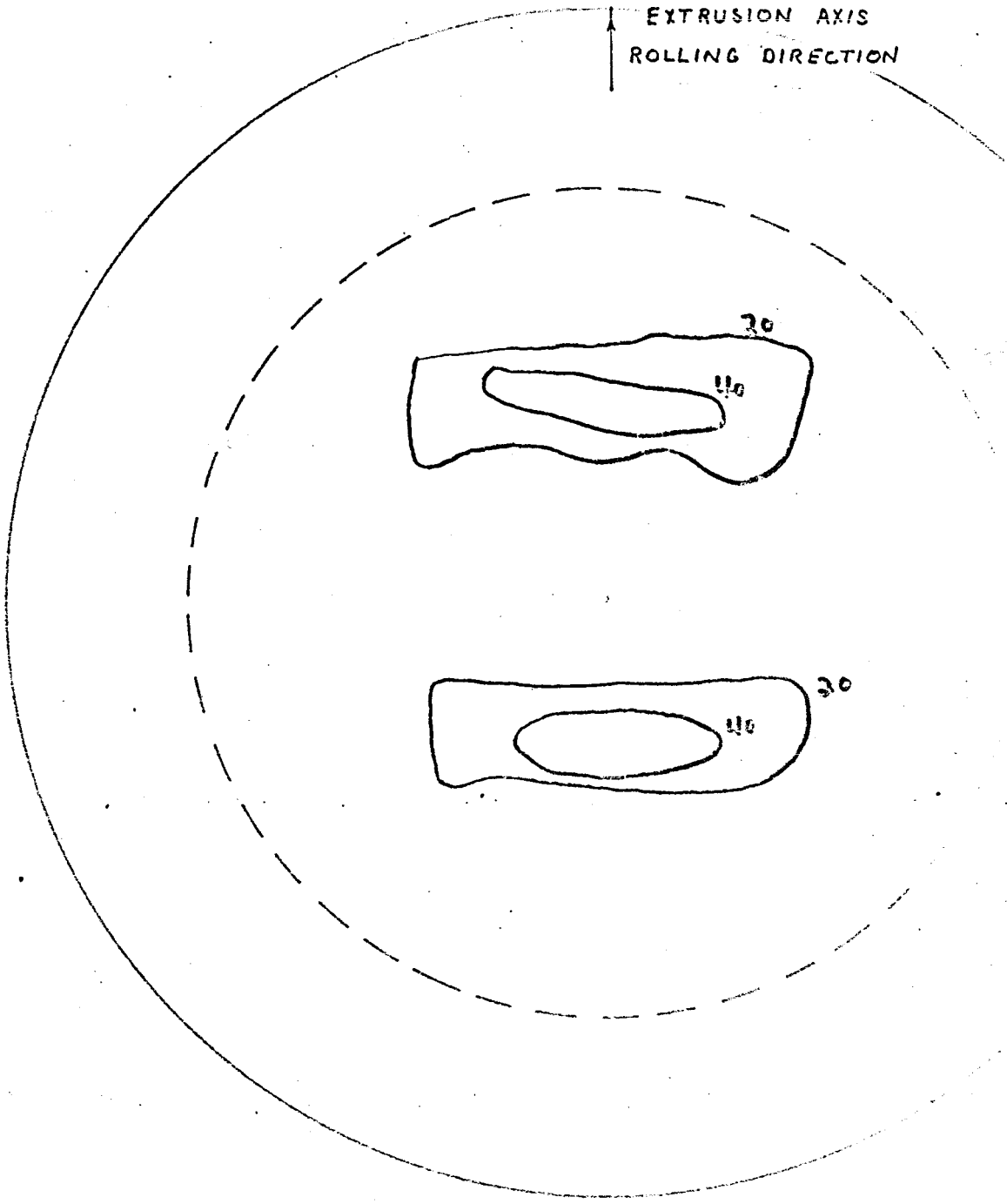

Figure 28. Pole Figure of As-Extruded TD Nickel Rolled 37% in Longitudinal Direction.

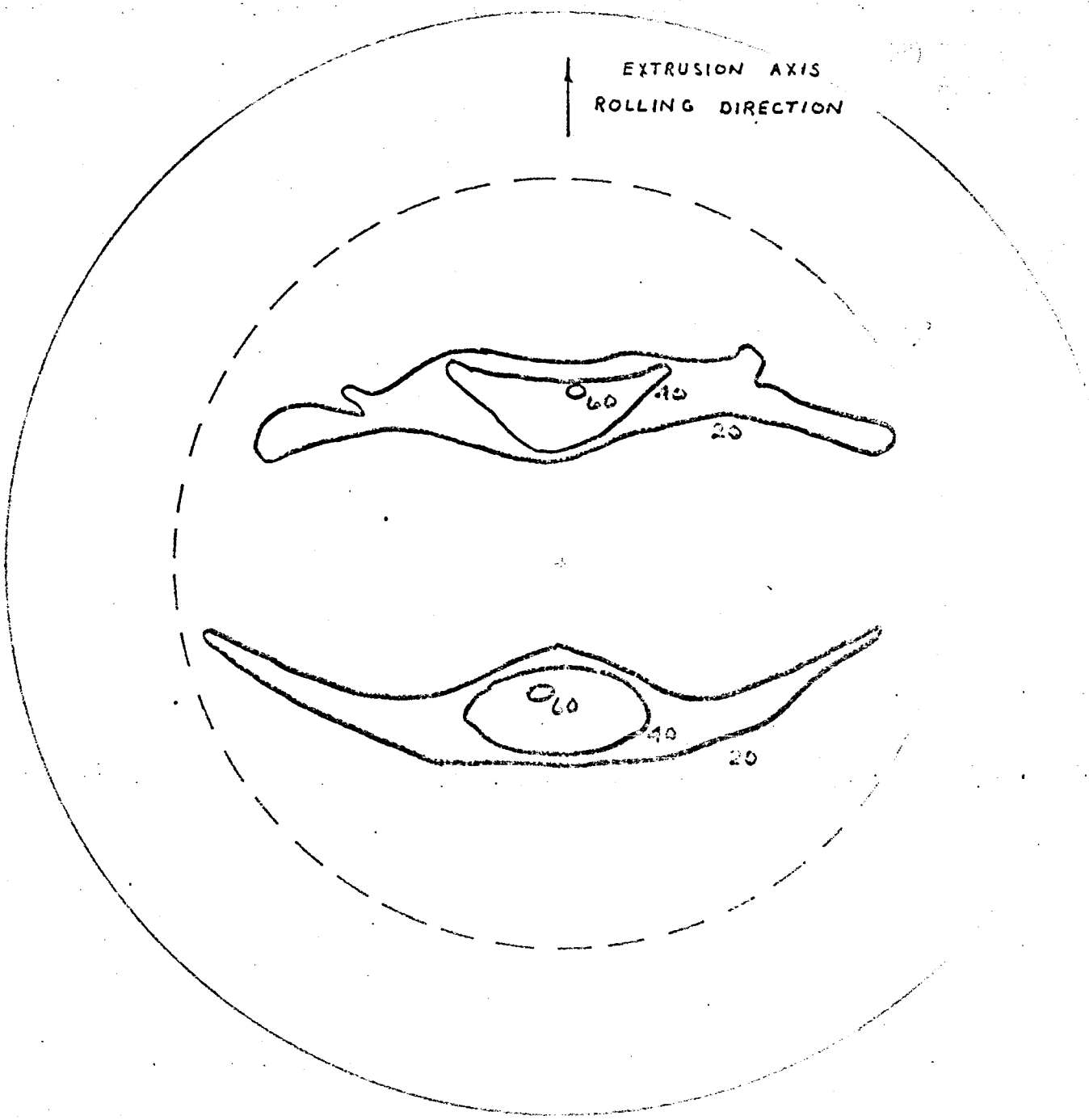

Figure 29. Pole Figure of As-Extruded TD Nickel Rolled 74% in Longitudinal Direction.

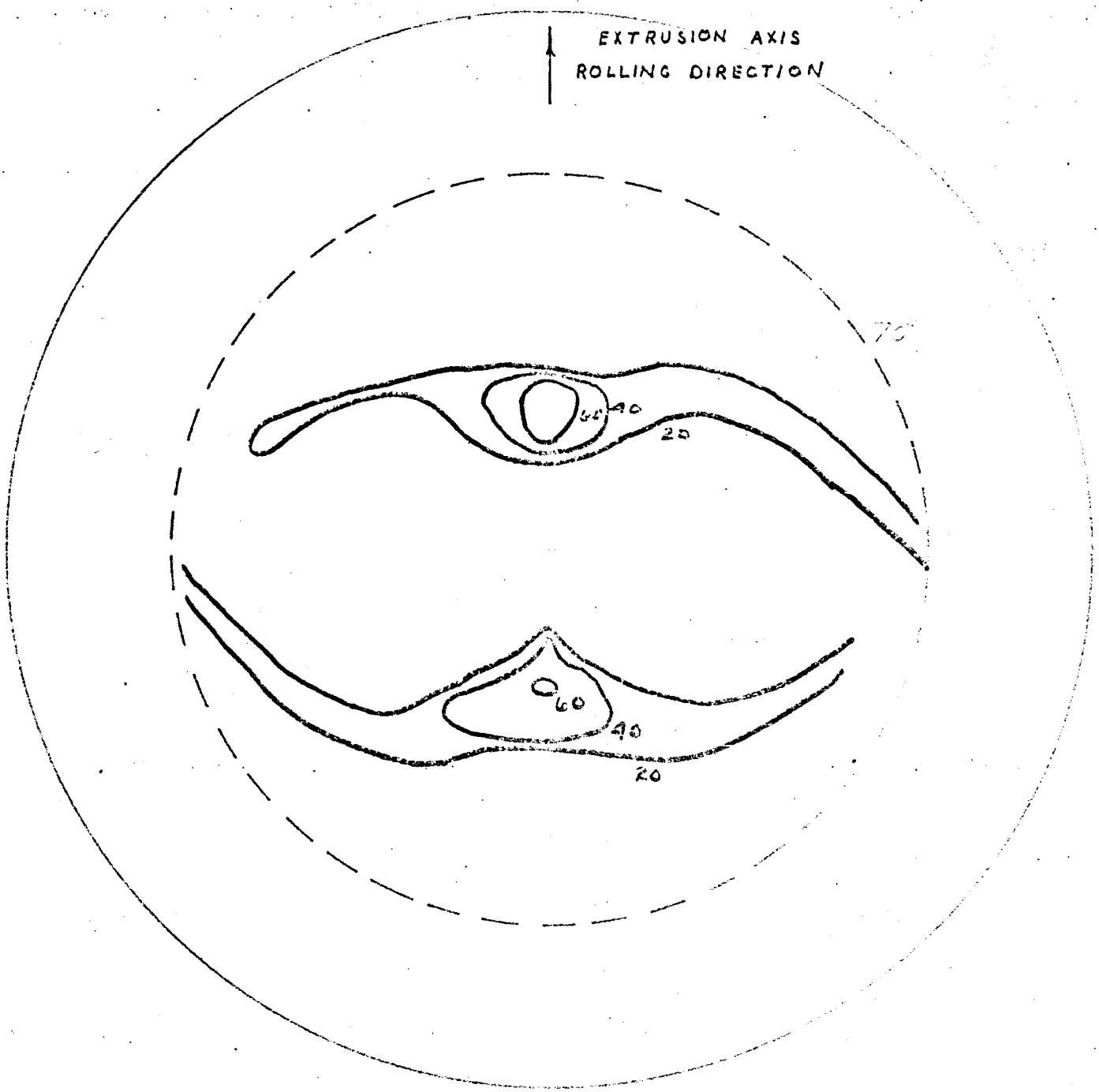

Figure 30. Pole Figure of As-Extruded TD Nickel Rolled 90% in Longitudinal Direction.

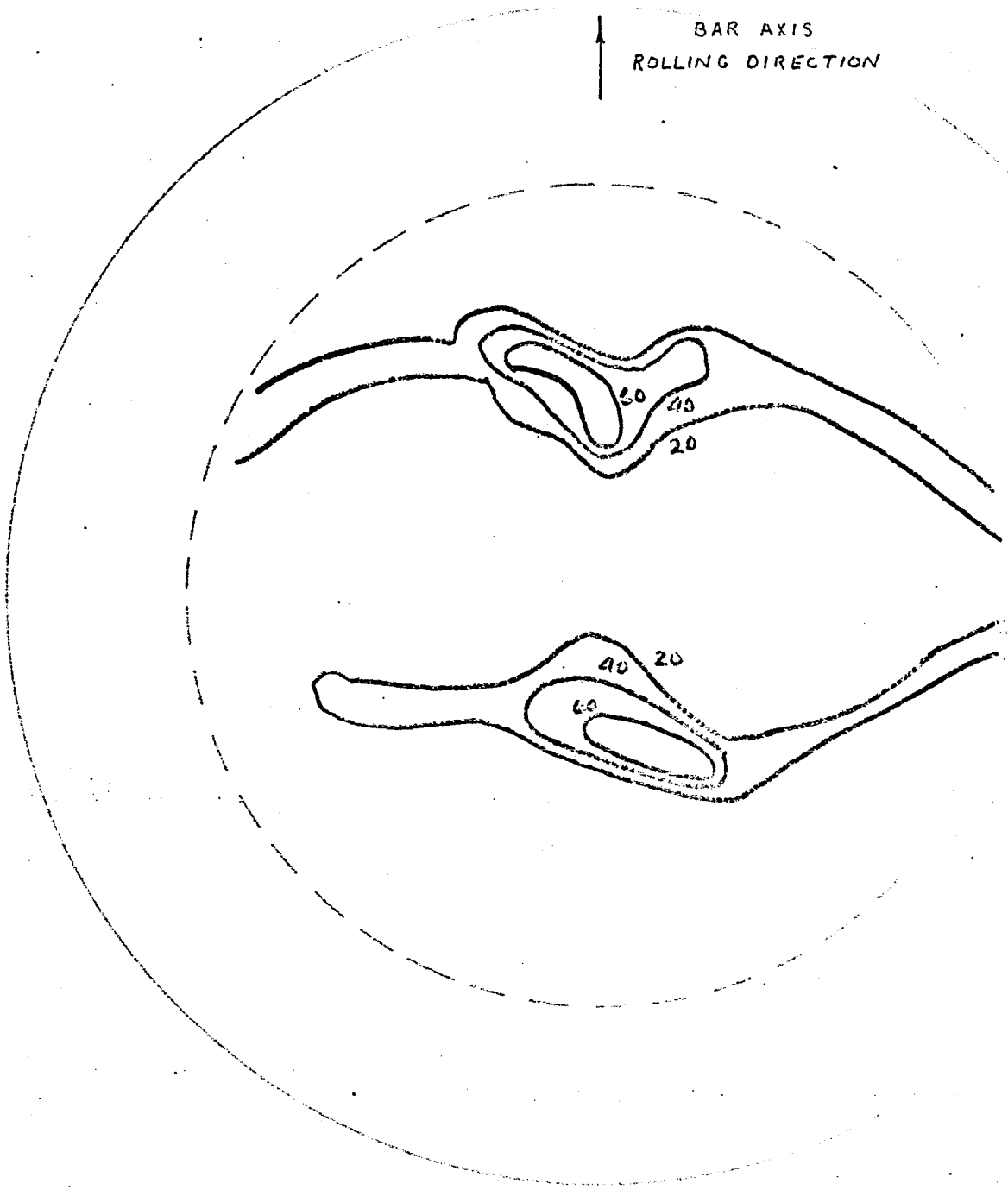

Figure 31. Pole Figure of Commercial TD Nickel Bar Rolled 87% in Longitudinal Direction.

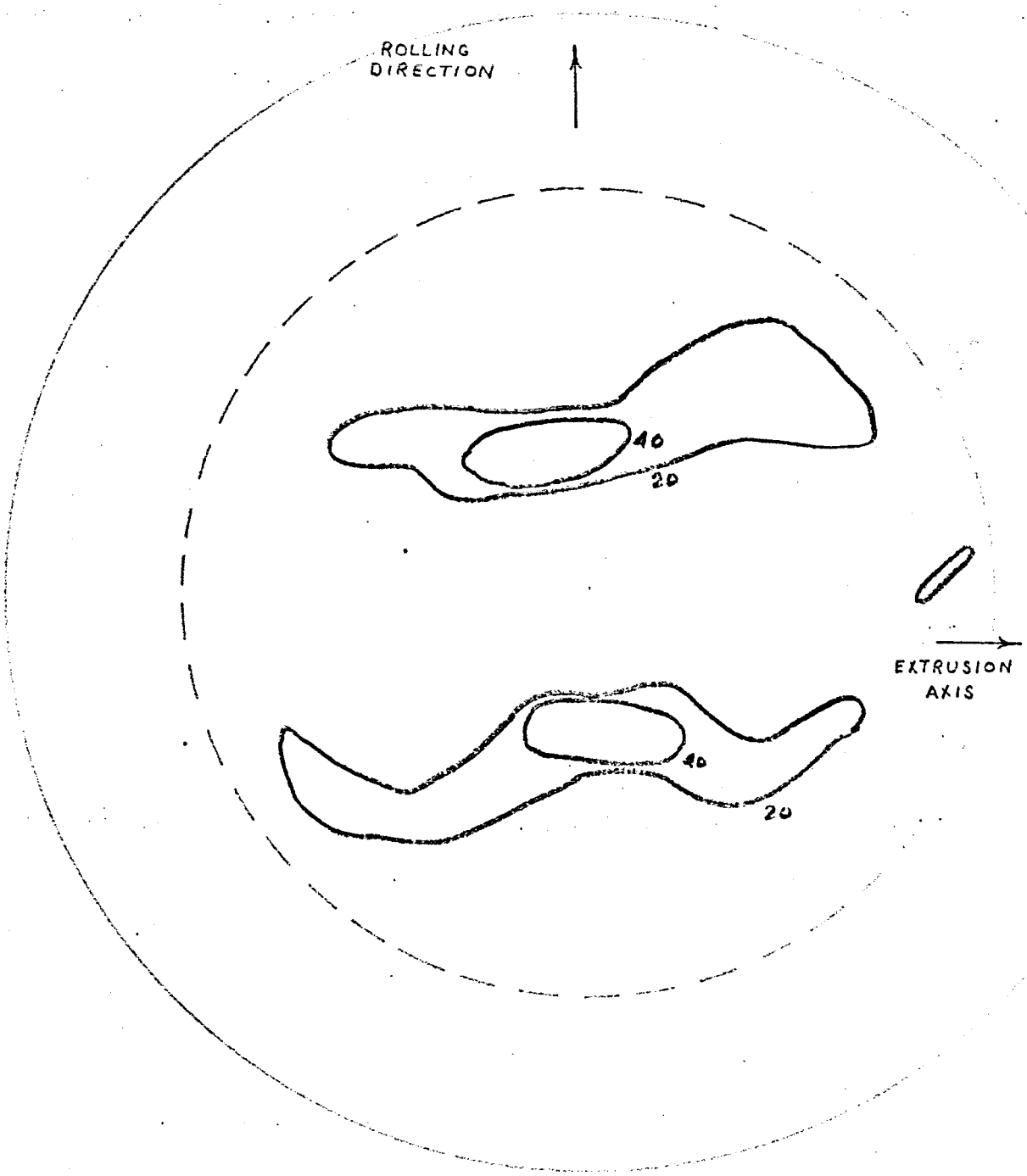

Figure 32. Pole Figure of As-Extruded TD Nickel Rolled 88% in Transverse Direction.

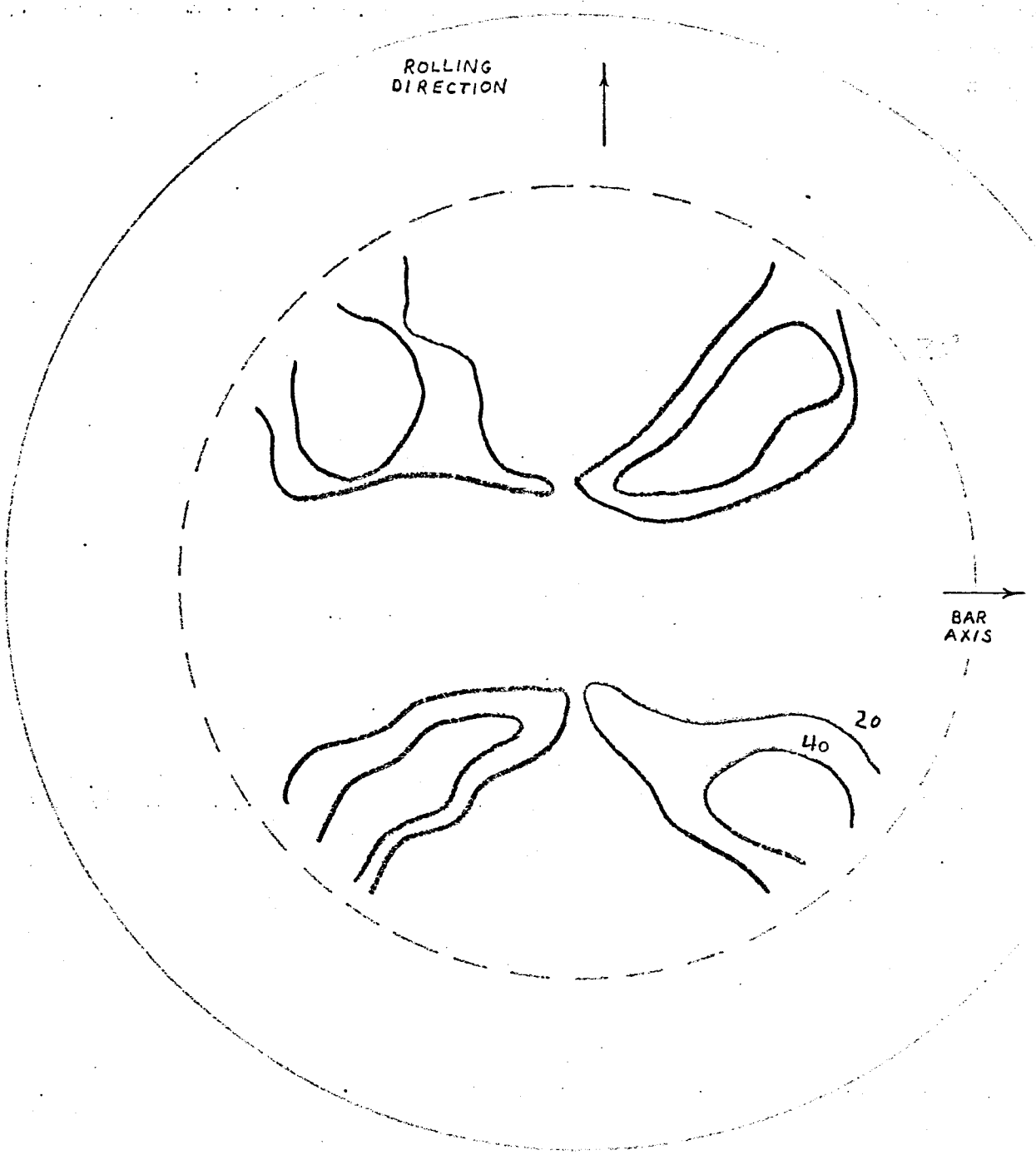

Figure 33. Pole Figure of Commercial TD Nickel Bar Rolled 87% in Transverse Direction.